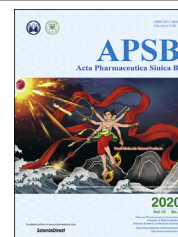




Chinese Pharmaceutical Association
Institute of Materia Medica, Chinese Academy of Medical Sciences

Acta Pharmaceutica Sinica B

www.elsevier.com/locate/apsb
www.sciencedirect.com



ORIGINAL ARTICLE

Exploring the hydrophobic channel of NNIBP leads to the discovery of novel piperidine-substituted thiophene[3,2-*d*]pyrimidine derivatives as potent HIV-1 NNRTIs



Dongwei Kang^a, Da Feng^a, Tiziana Ginex^c, Jinmi Zou^a, Fenju Wei^a, Tong Zhao^a, Boshi Huang^a, Yanying Sun^a, Samuel Desta^a, Erik De Clercq^b, Christophe Pannecouque^b, Peng Zhan^{a,*}, Xinyong Liu^{a,*}

^aDepartment of Medicinal Chemistry, Key Laboratory of Chemical Biology, Ministry of Education, School of Pharmaceutical Sciences, Shandong University, Jinan 250012, China

^bRega Institute for Medical Research, Laboratory of Virology and Chemotherapy, K.U. Leuven, Leuven B-3000, Belgium

^cDepartment of Nutrition, Food Science and Gastronomy, Faculty of Pharmacy, Campus Torribera, Institute of Biomedicine and Institute of Theoretical and Computational Chemistry, University of Barcelona, Santa Coloma de Gramenet 08921, Spain

Received 14 May 2019; received in revised form 25 July 2019; accepted 25 August 2019

KEYWORDS

HIV-1;
NNRTIs;
NNIBP;
Thiophene[3,2-*d*]
pyrimidine;
Hydrophobic channel

Abstract In this report, a series of novel piperidine-substituted thiophene[3,2-*d*]pyrimidine derivatives were designed to explore the hydrophobic channel of the non-nucleoside reverse transcriptase inhibitors binding pocket (NNIBP) by incorporating an aromatic moiety to the left wing of the lead **K-5a2**. The newly synthesized compounds were evaluated for anti-HIV potency in MT-4 cells and inhibitory activity to HIV-1 reverse transcriptase (RT). Most of the synthesized compounds exhibited broad-spectrum activity toward wild-type and a wide range of HIV-1 strains carrying single non-nucleoside reverse transcriptase inhibitors (NNRTI)-resistant mutations. Especially, compound **26** exhibited the most potent activity against wild-type and a panel of single mutations (L100I, K103N, Y181C, Y188L and E138K) with an EC₅₀ ranging from 6.02 to 23.9 nmol/L, which were comparable to those of etravirine (ETR). Moreover, the RT inhibition activity, preliminary structure–activity relationship and molecular docking were also investigated. Furthermore, **26** exhibited favorable pharmacokinetics (PK) profiles and with a bioavailability of 33.8%. Taken together, the results could provide valuable insights for further optimization

*Corresponding authors. Tel./fax: +86 531 88380270.

E-mail addresses: zhanpeng1982@sdu.edu.cn (Peng Zhan), xinyongl@sdu.edu.cn (Xinyong Liu).

Peer review under responsibility of Institute of Materia Medica, Chinese Academy of Medical Sciences and Chinese Pharmaceutical Association.

<https://doi.org/10.1016/j.apsb.2019.08.013>

2211-3835 © 2020 Chinese Pharmaceutical Association and Institute of Materia Medica, Chinese Academy of Medical Sciences. Production and hosting by Elsevier B.V. This is an open access article under the CC BY-NC-ND license (<http://creativecommons.org/licenses/by-nc-nd/4.0/>).

and compound **26** holds great promise as a potential drug candidate for the treatment of HIV-1 infection.

© 2020 Chinese Pharmaceutical Association and Institute of Materia Medica, Chinese Academy of Medical Sciences. Production and hosting by Elsevier B.V. This is an open access article under the CC BY-NC-ND license (<http://creativecommons.org/licenses/by-nc-nd/4.0/>).

1. Introduction

Acquired immune deficiency syndrome (AIDS) is caused by human immunodeficiency virus (HIV), which could enter the host cell and eventually leads to significant weakening of the host immune system. In the life cycle of HIV-1, reverse transcriptase (RT) is responsible for transcribing the single-stranded RNA genome to a double-stranded DNA, and it is a crucial target for development of novel anti-AIDS drugs¹. Among the HIV-1 RT inhibitors, non-nucleoside reverse transcriptase inhibitors (NNRTIs), due to their unique antiviral potency, high specificity and low toxicity, gained a definitive position in highly active antiretroviral therapy (HAART) regimens used to treat HIV-1^{2–4}.

Nevirapine (NVP), delavirdine (DLV), and efavirenz (EFV) were approved as the first-generation NNRTIs for AIDS therapy⁵. However, their low genetic barrier results in the emergence of drug-resistant mutants rapidly. K103N and Y181C are the two most prevalent mutations *in vivo*, which elicited frequently resistance to NVP and EFV⁶. Etravirine (**1**, ETR) and rilpivirine (**2**, RPV), both of which belong to the diarylpyrimidine (DAPY) family, were approved as the second-generation NNRTIs in 2008 and 2011 by U. S. Food and Drug Administration (FDA), respectively⁵. Although they could effectively inhibit most of the RT-resistant mutations caused by the first-generation NNRTIs, they generally failed to suppress the most refractory mutations E138K and RES056 (K103N + Y181C)^{7,8}. In addition, the patients treated with second-generation NNRTIs were frequently reported with hypersensitivity reactions and other adverse effects^{9,10}. Therefore, new NNRTIs that offer a combination of improved potency against these mutants, a favorable profile of safety and tolerability is urgently needed^{11–13}.

Previous research efforts in our lab led to the discovery of two potent HIV-1 NNRTIs, named as **K-5a2** and **25a** (Fig. 1), exhibiting excellent activities against drug-resistant mutations compared to that of ETR^{14,15}. Both compounds share a thiophene[3,2-*d*]pyrimidine central scaffold and a flexible extended right wing with piperidine-linked benzenesulfonamide structure, with the difference that **K-5a2** retains the 4-cyano-2,6-dimethylphenyl structure of ETR in the left wing while **25a**

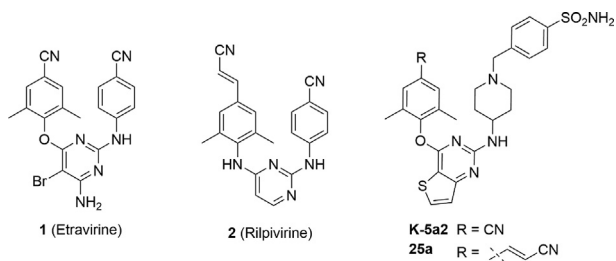


Figure 1 Chemical structures of second-generation NNRTI drugs and thiophene[3,2-*d*]pyrimidine lead **K-5a2** and **25a**.

features the 4-cyanovinyl-2,6-dimethylphenyl structure of RPV in its left wing. The co-crystal structures of wild-type (WT) and mutant HIV-1 RT in complex with **K-5a2** and **25a** indicated that they displayed potent activity against WT and a panel of NNRTI-resistant mutant HIV-1 strains due to conformational flexibility and positional adaptability of the inhibitors, and the network of main chain hydrogen bonds and hydrophobic interactions developed between the inhibitors and NNIBP. Especially, the hydrophobic interactions between the left wing of **K-5a2** and the hydrophobic channel surrounded by Tyr181, Tyr188, Phe227, Trp229, and Leu234 were critical for the enzyme–inhibitor complex formation. Although the 4-cyano-2,6-dimethylphenyl structure of **K-5a2** projected into the hydrophobic channel, it contacted with Tyr188 and Trp229 only and did not develop an effective π – π interaction with the highly conserved residue Phe227. As depicted in Fig. 2, we can learn that the hydrophobic channel still has enough space to accommodate structurally diverse groups^{16–18}.

In the present work, we paid our attention to explore the structure–activity relationship (SARs) of this underexplored region in the NNIBP by introducing different aromatic structures, including thiophene, furfuran and substituted benzene ring, to the left wing of **K-5a2**, with the aim to develop novel potent NNRTIs with improved drug resistance profiles. The synthetic routes, anti-HIV activity, preliminary SARs and modeling analysis of these novel thiophene[3,2-*d*]pyrimidine derivatives will be discussed.

2. Results and discussion

2.1. Chemistry

Schemes 1 and 2 illustrate the general synthetic routes of the intermediates **6a–k** and target compounds **11–32**. Firstly, Suzuki coupling of various boronic acid derivatives with commercially available 4-iodo-2,6-dimethylphenol (**5**), in DMF/H₂O solution using Pd(PPh₃)₄ as catalyst, provided the intermediates **6a–k** (Scheme 1). Compounds **6a–k** were followed by a nucleophilic substitution with 2,4-dichlorothiopheno[3,2-*d*]pyrimidine (**7**) in the presence of potassium carbonate to afford the intermediates **8a–k**, respectively. Then, the intermediates **9a–k** were obtained by Buchwald-Hartwig cross coupling reactions of **8a–k** with 4-(*tert*-butoxycarbonyl)-aminopiperidine in the presence of BINAP and PdCl₂(PPh₃)₂. Removing the Boc protecting group of **9a–k** by trifluoroacetic acid (TFA) furnished the key intermediates **10a–k**, which were reacted with 4-(bromomethyl)benzenesulfonamide or 4-(chloromethyl)benzamide to yield the target compounds **11–32** (Scheme 2).

2.2. *In vitro* anti-HIV activities

The newly synthesized derivatives **11–32** were firstly evaluated for their antiviral potency against WT HIV-1 (IIB) and a HIV-2

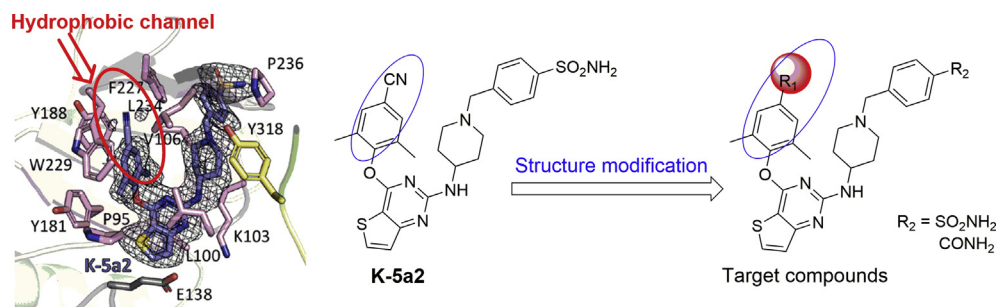
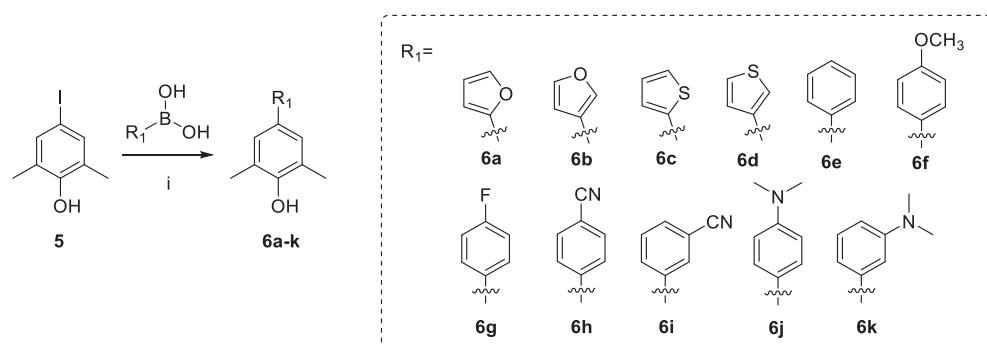
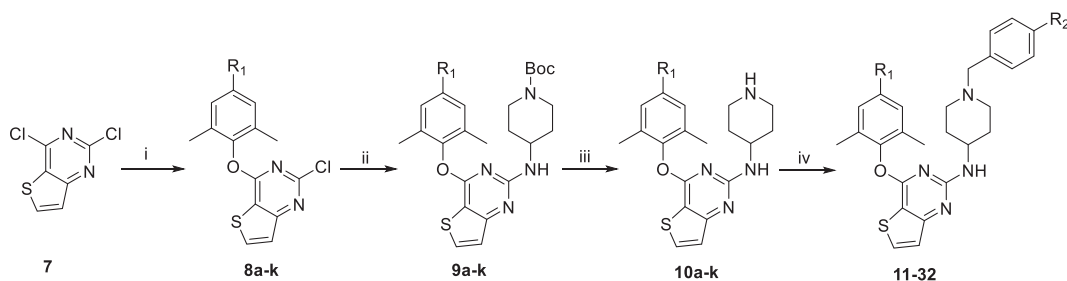


Figure 2 Design of the novel thiophene[3,2-*d*]pyrimidine derivatives.



Scheme 1 Synthesis of **6a–k**. Reagents and conditions: (i) Pd(PPh₃)₄, K₂CO₃, DMF, H₂O, 100 °C.



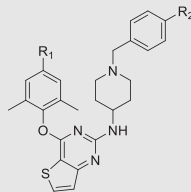
Scheme 2 Synthesis of the target compounds **11–32**. Reagents and conditions: (i) **6a–k**, DMF, K₂CO₃, r.t.; (ii) BINAP, PdCl₂(PPh₃)₂, Cs₂CO₃, *N*-(*tert*-butoxycarbonyl)-4-aminopiperidine, 1,4-dioxane, 120 °C; (iii) TFA, DCM, r.t.; (iv) 4-(bromomethyl) benzenesulfonamide or 4-(chloromethyl) benzamide, DMF, K₂CO₃, r.t.

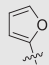
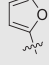
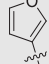
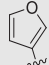
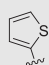
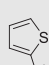
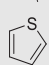
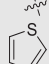

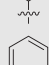
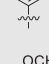
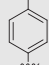
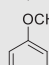
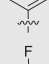
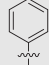
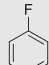
strain (ROD) in MT-4 cell cultures. NVP, EFV, ETR and the lead compound **K-5a2** were selected as control. The values of EC₅₀ (50% effective concentration), CC₅₀ (50% cytotoxic concentration), and SI (selectivity index, CC₅₀/EC₅₀ ratio) of the target compounds are summarized in Table 1.

As depicted in Table 1, all the target compounds exhibited effective potency against WT HIV-1 with EC₅₀ values ranging from 9.93 to 882 nmol/L. Among them, most compounds demonstrated EC₅₀ values of 9.93–93.3 nmol/L, which were superior to that of the control drug NVP (EC₅₀ = 186 nmol/L). Especially, compound **26** proved to be the most potent inhibitor against HIV-1 (IIIB) with an EC₅₀ value of 9.93 nmol/L, which was comparable to that of EFV (EC₅₀ = 5.25 nmol/L) and ETR (EC₅₀ = 5.03 nmol/L), but slightly weak to that of **K-5a2** (EC₅₀ = 1.4 nmol/L). Besides, compounds **11**, **23**, **24**, **25** and **27** were also endowed with promising anti-HIV-1 potencies (EC₅₀ = 17.7, 11.3, 12.8, 17.0 and 13.3 nmol/L, respectively) and

moderate cytotoxicity (CC₅₀ = 13.5, 16.9, 6.80, 5.31 and 14.0 μmol/L, respectively). In the case of HIV-2 (ROD), all the compounds showed weaker activity or lost activity.

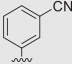
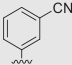
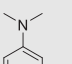
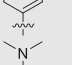
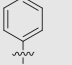
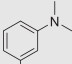
Preliminary investigation of the SARs revealed that the nature of the substituent group of the left wing (R₁) and right wing (R₂) have a significant effect on their antiviral potency. Detailed comparison of the activities of **11–18** suggested that the substitution position of thiophene and furfuran ring have little effect on their activity toward WT HIV-1 strain. However, a phenyl ring seems more favorable to the activity than a thiophene or furfuran ring at the R₁ position when comparing the activity of **11–18** (EC₅₀ = 17.7–240 nmol/L) and **19**, **20** (EC₅₀ = 43.8–47.7 nmol/L), which could be explained by the stronger stacking interaction between the phenyl moiety and resides in the hydrophobic channel of NNIBP. Elaboration with a F atom or CN substituents at the *para*-position of the phenyl ring yielded **23–26** with a highly effective potency of 9.93–17.0 nmol/L, while OCH₃ or N(CH₃)₂ substituents at this position (**21**, **22**, **29**,

Table 1 Anti-HIV-1 (IIIB) and HIV-2 (ROD) activity, cytotoxicity and SI of target compounds **11–32**.


Compd.	R ₁	R ₂	EC ₅₀ (nmol/L) ^a		CC ₅₀ (μmol/L) ^b	SI ^c	
			IIIB	ROD		IIIB	ROD
11		SO ₂ NH ₂	17.7 ± 4.83	4148 ± 1785	13.5 ± 3.94	762	3
12		CONH ₂	93.3 ± 82.8	25,289 ± 18,400	28.9 ± 15.6	310	1
13		SO ₂ NH ₂	63.6 ± 11.4	6805 ± 1225	15.6 ± 4.97	246	2
14		CONH ₂	57.5 ± 12.7	3181 ± 832	15.8 ± 7.04	275	5
15		SO ₂ NH ₂	49.5 ± 14.8	5111 ± 1707	21.5 ± 0.89	435	4
16		CONH ₂	203 ± 51.5	>20,535	≥20.5	≥101	NA ^d
17		SO ₂ NH ₂	31.6 ± 17.7	4802 ± 916	15.4 ± 5.86	489	3
18		CONH ₂	240 ± 94.3	>17,044	17.0 ± 12.9	71	<1
19		SO ₂ NH ₂	43.8 ± 15.6	6135 ± 272	21.3 ± 1.26	487	3
20		CONH ₂	47.7 ± 11.8	3842 ± 1765	17.5 ± 6.18	367	5
21		SO ₂ NH ₂	61.1 ± 10.3	>16,635	16.6 ± 4.65	272	<1
22		CONH ₂	52.6 ± 11.4	5035 ± 685	13.4 ± 5.94	256	3
23		SO ₂ NH ₂	11.3 ± 2.07	3283 ± 1255	16.9 ± 4.77	1492	5
24		CONH ₂	12.8 ± 2.73	≥5655	6.80 ± 3.13	532	<1
25		SO ₂ NH ₂	17.0 ± 5.78	5560 ± 42.3	5.31 ± 2.56	312	1
26		CONH ₂	9.93 ± 1.27	>5488	5.48 ± 2.12	552	<1

(continued on next page)

Table 1 (continued)

Compd.	R ₁	R ₂	EC ₅₀ (nmol/L) ^a		CC ₅₀ (μmol/L) ^b	SI ^c	
			IIIB	ROD		IIIB	ROD
27		SO ₂ NH ₂	13.3 ± 2.60	4916 ± 2247	14.0 ± 8.28	1054	3
28		CONH ₂	23.4 ± 16.9	>4169	4.16 ± 1.75	178	<1
29		SO ₂ NH ₂	79.2 ± 48.7	>18,381	18.3 ± 4.50	232	<1
30		CONH ₂	176 ± 26.4	>23,535	23.5 ± 0.38	134	<1
31		SO ₂ NH ₂	882 ± 323	>110,175	110 ± 1.46	125	<1
32		CONH ₂	163 ± 57.8	4659 ± 824	19.8 ± 4.47	121	4
NVP	—	—	186 ± 59.0	>9510	>9.51	>51	NA ^d
EFV	—	—	5.25 ± 1.98	>5330	>6.33	>1205	NA ^d
ETR	—	—	5.03 ± 1.68	>4594	>4.59	>913	NA ^d
K-5a2 ^e	—	—	1.4 ± 0.4	≥227,890	≥227	>159,101	NA ^d

^aEC₅₀: concentration of compound required to achieve 50% protection of MT-4 cell cultures against HIV-1-induced cytotoxicity, as determined by the MTT method. A smaller EC₅₀ values means that the compound has greater activity.

^bCC₅₀: concentration required to reduce the viability of mock-infected cell cultures by 50%, as determined by the MTT method. A larger CC₅₀ values means that the compound has lower toxicity.

^cSI: selectivity index, the ratio of CC₅₀/EC₅₀.

^dNA: stands for ≥1 or <1.

^eData were reported in ref. 14. —Not applicable.

30, EC₅₀ = 52.6–176 nmol/L) resulted in a decreased activity, suggesting that the antiviral activity is very sensitive to the kind of the substituents. Furthermore, by comparing the activity of **25–28** with **29–32**, we concluded that the position of CN and N(CH₃)₂ substituents has little effect on the activity. In addition, the effect of the type of substituent (SO₂NH₂ and CONH₂) in the right wing on the antiviral activity was not obvious.

All the compounds were further evaluated against a panel of clinically relevant NNRTIs-resistant single-mutant strains (L100I, K103N, Y181C, Y188L, E138K) and double-mutant strains F227L + V106A, RES056. The results were depicted in Table 2. Moreover, the SI and RF (fold-resistance factor, EC₅₀ mutant strain/EC₅₀ WT strain) were summarized in Table 3. In general, the compounds activity to mutant strains exhibits a similar trend to their potency to WT HIV-1 strain. Compound **26** demonstrated the most active potency toward all the single-mutant HIV-1 strain, including L100I, K103N, Y181C, Y188L and E138K (EC₅₀ = 10.5, 6.02, 18.9, 23.9 and 23.2 nmol/L, respectively), its activity was superior to that of NVP and EFV, and comparable to that of ETR. Interestingly, all the target compounds displayed lower fold resistance (FR, ratio of EC₅₀ against mutant strain/EC₅₀ against WT strain) values toward K103N than other mutant strains. Most compounds were demonstrated with improved activity against K103N mutation compared to WT strain. For

example, **26** displayed the most effective activity against K103N (EC₅₀ = 6.02 nmol/L, FR = 0.6), being more potent than its activity to WT HIV-1 (EC₅₀ = 9.93 nmol/L). For double-mutant HIV-1 strain F227L + V106A, compounds **23** and **27** were proved to be the most potent inhibitors and exhibited EC₅₀ values of 46.6 and 49.2 nmol/L, respectively, being far more potent than NVP (EC₅₀ > 9510 nmol/L) and EFV (EC₅₀ = 268 nmol/L), and comparable to ETR (EC₅₀ = 14.2 nmol/L). In the case of RES056, which is the most challenging double mutation emerging in HIV patients, compounds **25** and **26** provided the greatest potency with EC₅₀ values of 103 and 125 nmol/L respectively, being superior to EFV (EC₅₀ = 265 nmol/L), but slightly inferior to ETR (EC₅₀ 42.5 nmol/L) and **K-5a2** (EC₅₀ = 30.6 nmol/L).

With the aim to validate the binding target of these novel piperidine-substituted thiophene[3,2-*d*]pyrimidine derivatives, their inhibitory effects on WT HIV-1 RT were investigated. As shown in Table 4, most compounds exhibited effective inhibitory activity (IC₅₀ = 0.161–0.624 μmol/L) to HIV-1 RT, being comparable to the lead **K-5a2** (IC₅₀ = 0.300 μmol/L), superior to the reference drug NVP (IC₅₀ = 1.220 μmol/L) and inferior to ETR (IC₅₀ = 0.011 μmol/L). Compound **31**, the weakest inhibitor of WT HIV-1 strain in cell culture (EC₅₀ = 882 nmol/L), exhibited the lowest binding-affinity for WT HIV-1 RT

Table 2 Activity against mutant HIV-1 strains of target compounds **11–32**.

Compd.	EC ₅₀ (nmol/L) ^a						
	L100I	K103N	Y181C	Y188L	E138K	F227L + V106A	RES056
11	89.3 ± 23.0	20.7 ± 2.75	63.5 ± 8.75	53.4 ± 2.15	49.9 ± 0.35	85.7 ± 9.71	565 ± 22.5
12	414 ± 37.9	129 ± 5.87	511 ± 77.2	307 ± 58.2	287 ± 4.98	1108 ± 269	2903 ± 119
13	186 ± 29.4	62.9 ± 10.4	197 ± 16.1	133 ± 3.35	193 ± 14.8	358 ± 18.4	1194 ± 184
14	262 ± 75.0	74.8 ± 2.93	180 ± 33.4	222 ± 30.5	177 ± 2.93	525 ± 21.1	813 ± 177
15	97.9 ± 62.4	23.1 ± 2.56	91.7 ± 18.2	106 ± 43.6	124 ± 88.7	56.7 ± 16.2	999 ± 151
16	731 ± 274	184 ± 90.2	731 ± 198	619 ± 3.59	662 ± 58.4	1092 ± 226	10,011 ± 1066
17	76.0 ± 17.2	17.9 ± 1.51	63.2 ± 16.1	62.0 ± 5.83	52.5 ± 11.3	56.8 ± 3.85	932 ± 88.4
18	925 ± 286	171 ± 56.9	741 ± 154	628 ± 49.6	739 ± 318	854 ± 186	4515 ± 1447
19	344 ± 117	59.9 ± 6.01	167 ± 24.5	121 ± 9.19	107 ± 18.8	200 ± 10.4	1713 ± 473
20	416 ± 87.9	102 ± 2.50	196 ± 54.6	205 ± 13.6	146 ± 12.5	395 ± 5.14	1733 ± 5.51
21	169 ± 2.91	57.6 ± 0.67	157 ± 5.61	146 ± 44.7	114 ± 9.20	122 ± 59.9	1563 ± 1280
22	268 ± 103	58.4 ± 7.14	158 ± 27.3	110 ± 3.57	149 ± 42.0	297 ± 39.8	1123 ± 353
23	45.4 ± 5.26	11.7 ± 1.03	44.8 ± 5.26	51.8 ± 8.47	30.9 ± 5.26	46.6 ± 15.5	388 ± 76.2
24	61.1 ± 9.35	11.7 ± 1.09	36.1 ± 1.21	51.4 ± 9.60	34.8 ± 10.6	56.6 ± 13.7	575 ± 120
25	27.4 ± 4.41	13.2 ± 0.33	30.8 ± 0.11	53.6 ± 3.50	44.4 ± 3.62	59.9 ± 0.11	103 ± 3.39
26	10.5 ± 4.56	6.02 ± 0.84	18.9 ± 2.28	23.9 ± 2.40	23.2 ± 8.64	97.2 ± 25.3	125 ± 39.3
27	24.6 ± 4.97	8.56 ± 1.69	32.4 ± 4.07	54.7 ± 2.26	34.8 ± 9.28	49.2 ± 8.26	347 ± 75.9
28	50.2 ± 10.3	20.0 ± 1.20	51.6 ± 4.32	73.4 ± 5.16	41.9 ± 4.56	157 ± 6.60	402 ± 41.9
29	247 ± 4.50	97.2 ± 3.07	260 ± 30.2	269 ± 30.0	183 ± 19.4	140 ± 1.31	1682 ± 388
30	1115 ± 543	173 ± 46.3	585 ± 33.3	556 ± 57.4	245 ± 173	1253 ± 804	>23,535
31	2401 ± 256	685 ± 0.21	2300 ± 413	1992 ± 46.5	979 ± 185	2157 ± 298	29,610 ± 4817
32	1135 ± 99.2	212 ± 7.34	626 ± 39.2	552 ± 45.6	198 ± 34.2	783 ± 196	4298 ± 1542
NVP	1403 ± 828	7818 ± 556	>9510	>9510	115 ± 24.5	>9510	>9510
EFV	46.5 ± 9.11	111 ± 35.4	6.33 ± 1.06	306 ± 53.9	5.12 ± 1.28	268 ± 48.7	265 ± 47.9
ETR	6.35 ± 1.77	3.13 ± 0.42	12.2 ± 2.63	17.3 ± 5.53	8.07 ± 2.52	14.2 ± 5.14	42.5 ± 15.1
K-5a2^b	3.4 ± 0.6	2.9	3.2 ± 0.4	3.0 ± 0.1	2.9	4.2 ± 1.2	30.6 ± 12

^aEC₅₀: concentration of compound required to achieve 50% protection of MT-4 cell cultures against HIV-1-induced cytotoxicity, as determined by the MTT method.

^bData were reported in Ref. 14.

Table 3 SI and RF values of target compounds **11–32**.

Compd.	SI (RF) ^a						
	L100I	K103N	Y181C	Y188L	E138K	F227L + V106A	RES056
11	151 (5.0)	651 (1.2)	213 (3.6)	253 (3.0)	271 (2.8)	158 (4.8)	24 (31.9)
12	70 (4.4)	224 (1.4)	57 (5.5)	94 (3.3)	101 (3.1)	26 (11.9)	10 (31.1)
13	84 (2.9)	249 (1.0)	79 (3.1)	117 (2.1)	81 (3.0)	44 (5.6)	13 (18.8)
14	60 (4.6)	212 (1.3)	88 (3.1)	71 (3.9)	89 (3.1)	30 (9.1)	19 (14.1)
15	220 (2.0)	932 (0.5)	235 (1.9)	203 (2.1)	173 (2.5)	380 (1.1)	22 (20.2)
16	≥28 (3.6)	≥111 (0.9)	≥28 (3.6)	≥33 (3.0)	≥31 (3.3)	≥19 (5.4)	≥2 (49.2)
17	203 (2.4)	865 (0.6)	245 (2.0)	249 (2.0)	295 (1.7)	272 (1.8)	17 (29.5)
18	18 (3.8)	99 (0.7)	23 (3.1)	27 (2.6)	23 (3.1)	20 (3.6)	4 (18.8)
19	62 (7.9)	356 (1.4)	127 (3.8)	176 (2.8)	200 (2.4)	106 (4.6)	12 (39.1)
20	42 (8.7)	171 (2.1)	89 (4.1)	85 (4.3)	120 (3.1)	44 (8.3)	10 (36.3)
21	98 (2.8)	289 (0.9)	105 (2.6)	114 (2.4)	145 (1.9)	136 (2.0)	11 (25.6)
22	50 (5.1)	230 (1.1)	85 (3.0)	122 (2.1)	90 (2.8)	45 (5.7)	12 (21.4)
23	372 (4.0)	1441 (1.0)	377 (4.0)	326 (4.6)	547 (2.7)	363 (4.1)	43 (34.3)
24	111 (4.8)	578 (0.9)	189 (2.8)	132 (4.0)	195 (2.7)	120 (4.4)	12 (44.9)
25	194 (1.6)	403 (0.8)	173 (1.8)	99 (3.2)	120 (2.6)	89 (3.5)	51 (6.1)
26	521 (1.1)	910 (0.6)	290 (1.9)	229 (2.4)	236 (2.3)	56 (9.8)	44 (12.6)
27	569 (1.9)	1639 (0.6)	432 (2.4)	256 (4.1)	402 (2.6)	285 (3.7)	40 (26.1)
28	83 (2.1)	208 (0.9)	81 (2.2)	57 (3.1)	99 (1.8)	26 (6.7)	10 (17.2)
29	74 (3.1)	189 (1.2)	71 (3.3)	68 (3.4)	100 (2.3)	131 (1.8)	11 (21.2)
30	21 (6.3)	135 (1.0)	40 (3.3)	42 (3.2)	96 (1.4)	19 (7.1)	<1 (>133)
31	46 (2.7)	161 (0.8)	48 (2.6)	55 (2.3)	112 (1.1)	51 (2.4)	4 (33.5)
32	17 (6.9)	93 (1.3)	32 (3.8)	36 (3.4)	100 (1.2)	25 (4.8)	5 (26.2)
NVP	>7 (7.5)	>1 (42)	NA (>51.1)	NA (>51)	>82 (0.6)	NA (>51.1)	NA (>51.1)
EFV	>136 (8.8)	>57 (21)	>1000 (1.2)	>21 (58)	>1237 (1.0)	>24 (51.1)	>24 (51.0)
ETR	>723 (1.3)	>1463 (0.6)	>376 (2.4)	>264 (3.5)	>569 (1.6)	>322 (2.8)	>108 (8.4)

^aRF is the ratio of EC₅₀ (resistant viral strain)/EC₅₀ (wild-type viral strain).

($IC_{50} = 1.681 \mu\text{mol/L}$). In general, the enzyme inhibitory activity (IC_{50}) of these novel synthesized compounds was consistent with their anti-HIV-1 (IIIB) activity (EC_{50}), and there was a good linear relationship between them (Fig. 3). All the results indicated that these novel synthesized piperidine-substituted thiophene[3,2-*d*]pyrimidine derivatives are classical NNRTIs.

2.3. Molecular modelling studies

Classical molecular dynamics (MD) simulations and MM/GBSA free energy calculations were performed to identify the molecular determinants responsible of the activity profile of the most effective inhibitor **26** bound to the WT and the mutated forms of HIV-1 RT. To this end, the X-ray crystal structure of the WT HIV-1 RT (PDB code: 6c0n), and its K103N (PDB code: 6c0o) and RES056 (K103N/Y181C) (PDB code: 6c0r) variants were used¹⁶. The co-crystallized NNRTIs **K-5a2** was used as template to place **26** into the inhibitor's binding site, according to the close similarity between the crystallographic and simulated ligands.

As depicted in Fig. 4, compound **26** adopts a horseshoe-like conformation in the NNIBP, which was commonly observed in

most DAPY NNRTIs. The complexes of **26** with WT, K103N or RES056 RT display the following common interactions: (i) the newly introduced biphenyl structure is stably accommodated into the hydrophobic channel and stabilized by π -stacking interactions with Y/C181, Y188, F227, and W229; (ii) the thiophene ring of **26** is projected towards the NNIBP entrance channel surrounded by V179 and E138; and (iii) the piperidine-linked benzamide structure of the right wing occupies the tolerant region I surrounded by K/N103, K104, V106, and F227.

The stability of the three protein–ligand complexes formed by **26** with the WT HIV-1 RT, mutant HIV-1 K103N and RES056 RT was analysed by means of 100 ns MD simulations. Final geometries for the three simulated systems are shown in Fig. 4. All the simulated systems were stable during MD simulation, as demonstrated by the root-mean square deviation (RMSD) values (Supporting Information Fig. S1A, B and C) for both the ligand and the residues that shape the NN binding site.

Accordingly to the binding mode, the $-\text{NH}$ guanidine group of the ligand is hydrogen-bonded to the backbone oxygen of K101 with average (K101) $\text{C}=\text{O}\cdots\text{HN}$ (**26**) distances of 2.4 ± 0.5 , 2.3 ± 0.5 and $3.2 \pm 0.5 \text{ \AA}$ respectively for the WT RT, and its single and double mutated variants (Fig. S1D, E and F) calculated along the last 30 ns of the MD trajectory. The protonated pyrimidine nitrogen of **26** is also involved in hydrogen-bonding with the backbone oxygen of K/N103 with average (K/N103) $\text{C}=\text{O}\cdots\text{HN}$ (**26**) distances of 2.5 ± 0.5 , 2.3 ± 0.5 and $4.1 \pm 0.6 \text{ \AA}$ respectively for the WT, singly and doubly mutated species (Fig. S1D, E and F).

In the hydrophobic channel of NNIBP, the benzonitril moiety of **26** stacks against Y188 and F227 (Fig. 4) with average distances of (Y188/P227) $4.4 \pm 0.6/3.3 \pm 0.6 \text{ \AA}$ for WT RT, $3.9 \pm 0.4/3.4 \pm 0.6 \text{ \AA}$ for the K103N variant, and $4.5 \pm 0.7/4.7 \pm 0.7 \text{ \AA}$ for the K103N/Y181C mutated enzyme (Fig. S1G, H and I). The involvement of F227 is allowed by the rearrangement of its side chain during the second part of the MD simulations.

As noted in the Experimental Section of this work, a similar ($EC_{50} = 9.93$ and 6.02 nmol/L) inhibitory activity was found by **26** in the WT and the single mutant K013N, whereas it was 20-fold less potent ($EC_{50} = 125 \text{ nmol/L}$) against the double mutant RES056. This last data could be explained by the gradual displacement of the ligand within the NNIBP observed during the MD simulation. This gradual displacement allowed the insertion of a water molecule with a consequent weakening of the (K101) $\text{C}=\text{O}\cdots\text{HN}$ (**26**) hydrogen–bonding interaction (Fig. S1F). Furthermore, the benzonitrile moiety slightly deviates from the optimal orientation required for the π -stacking interaction with Y188 and F227 in the hydrophobic channel. All these factors would contribute to the reduced activity of **26** against RES056. Indeed, the structural destabilization observed for RES056 in complex with **26** was confirmed by MM/GBSA free energy calculations performed on the last 30 ns for the previously generated MD trajectories. In this regard, binding affinities (ΔG_{bind}) of -73.4 and -74.1 kcal/mol were obtained respectively for the WT HIV-1 RT and the K103N mutant (Table 5), whereas a binding free energy of -65.9 kcal/mol was observed for **26** in the NNIBP of the double mutant RES056.

2.4. In vivo pharmacokinetics (PK) study and acute toxicity assessment

Our study was approved by the ethics committee of Cheeloo College of Medicine, Shandong University (Jinan, China). All procedures

Table 4 Inhibitory activity against WT HIV-1 RT of target compounds **11–32**.

Compd.	IC_{50} ($\mu\text{mol/L}$) ^a	Compd.	IC_{50} ($\mu\text{mol/L}$) ^a
11	0.243 ± 0.037	22	0.233 ± 0.028
12	0.901 ± 0.045	23	0.211 ± 0.015
13	0.265 ± 0.059	24	0.171 ± 0.010
14	0.249 ± 0.001	25	0.288 ± 0.026
15	0.227 ± 0.046	26	0.182 ± 0.016
16	0.595 ± 0.044	27	0.207 ± 0.006
17	0.167 ± 0.014	28	0.202 ± 0.020
18	0.624 ± 0.055	29	0.477 ± 0.009
19	0.164 ± 0.005	30	0.473 ± 0.059
20	0.161 ± 0.014	31	1.681 ± 0.056
21	0.268 ± 0.052	32	0.271 ± 0.016
NVP	1.220 ± 0.337	ETR ^b	0.011 ± 0.000
EFV ^b	0.030 ± 0.000	K-5a2 ^b	0.300 ± 0.060

^a IC_{50} : inhibitory concentration of test compound required to inhibit biotin deoxyuridine triphosphate (biotindUTP) incorporation into WT HIV-1 RT by 50%.

^bThe data were obtained from the same laboratory with the same method (Prof. Erik De Clercq, Rega Institute for Medical Research, KU Leuven, Belgium).

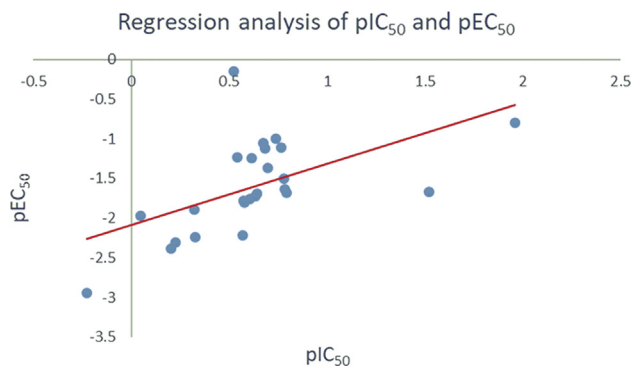


Figure 3 Regression analysis of pIC_{50} and pEC_{50} values for the newly synthesized derivatives.

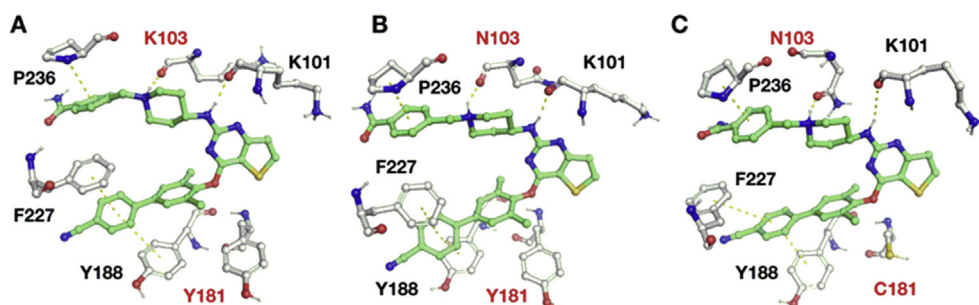


Figure 4 Final geometries for **26** in complexes with WT (A), K103N (B) and RES056 (C) RT. Hydrogen-bonding interactions for the $-NH$ guanidine group and the protonated nitrogen atom with K101 and K103 of the protein as well as the π -stacking with F227 and Y188 are also highlighted.

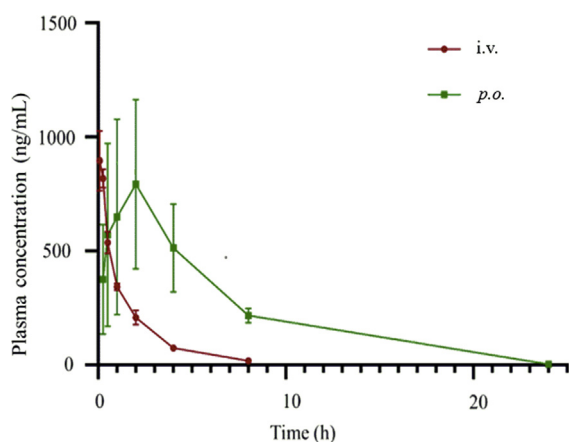


Figure 5 The plasma concentration–time profiles of **26** in Wistar rat following *p.o.* administration (20 mg/kg) and *i.v.* administration (2 mg/kg).

performed in studies were in accordance with the ethical standards of the institution or practice at which the studies were conducted. The *in vivo* pharmacokinetic profile of compound **26** was examined in Wistar rat PK model (Fig. 5 and Table 6). After a single 2 mg/kg *i.v.* dose, **26** was characterized by a modest clearance ($CL = 25.0$ mL/min/kg), a short terminal half-life ($t_{1/2} = 1.71$ h) and a maximum concentration (C_{max}) of 941 ng/mL. When administered at 20 mg/kg orally, compound **26** was rapidly absorbed with a T_{max} of 2.00 h, a favorable half-life of 2.68 h, and a C_{max} of 762 ng/mL. The oral bioavailability (F) was 33.8%, which was sufficiently enough for a drug candidate.

Furthermore, **26** was performed acute toxicity experiment in Kunming mice. As depicted in Fig. 6, no mortality or poisoning symptom was found after given the mice with single oral doses of

2000 mg/kg. Besides, there have no significant weight and behaviors changes compared to the control group during the post-treatment period of 8 days.

3. Conclusions

In conclusion, we designed and synthesized a novel series of piperidine-substituted thiophene[3,2-*d*]pyrimidine derivatives by incorporating an aromatic moiety to interact with the hydrophobic channel of NNIBP. These compounds showed effective potency against WT and most of NNRTIs-resistant HIV-1 strain, especially to the challenging K103N mutation. Compound **26** turns out as the most potent inhibitor with EC_{50} values of 9.93, 10.5, 6.02, 18.9, 23.9 and 23.2 nmol/L against WT, L100I, K103N, Y181C, Y188L and E138K strains, respectively, being comparable to those of ETR. Furthermore, **26** also exerted stronger binding affinity for WT HIV-1 RT with an IC_{50} value of 0.182 μ mol/L. Molecular simulation provides a reasonable explanation why **26** exhibited different activity against a panel of HIV-1 mutant strains. Notably, **26** exhibited favorable PK profiles, with a moderate clearance in rats and its bioavailability is up to 33.8%. Taken together, the results will contribute to explore the hydrophobic channel of NNIBP for developing novel potent NNRTIs and compound **26** holds great promise as a potential drug candidate for the treatment of HIV-1 infection.

4. Experimental

4.1. Chemistry

All melting points were determined on a micro melting point apparatus (YRT-3, Tianjin, China) and are uncorrected. 1H NMR and ^{13}C NMR spectra were recorded in $CDCl_3$ or $DMSO-d_6$ on a Bruker AV-400 spectrometer (Zurich, Switzerland) with tetramethylsilane (TMS) as the internal standard. A G1313A Standard LC

Table 5 MM/GBSA^a calculations for the three MD simulated systems. Values are expressed in kcal/mol.

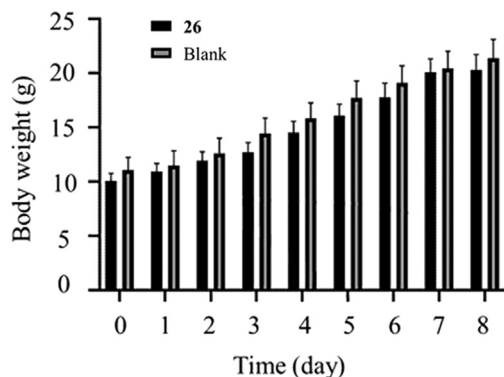
System	E_{vdw}	E_{elect}	ΔG_{gas}	E_{GB}	E_{SURF}	ΔG_{solv}	ΔG_{bind}
WT+26	-87.2 ± 4.3	-2.9 ± 8.8	-90.1 ± 10.8	26.2 ± 8.8	-9.6 ± 0.2	16.6 ± 8.7	-73.4 ± 4.7
K103N + 26	-88.2 ± 3.3	-39.3 ± 9.2	-127.4 ± 9.8	62.0 ± 9.3	-9.5 ± 0.2	52.5 ± 9.3	-74.1 ± 3.9
RES056 + 26	-3.1 ± 3.4	-35.2 ± 13.3	-118.2 ± 14.4	62.1 ± 13.1	-9.6 ± 0.2	52.4 ± 13.0	-65.9 ± 3.8

E_{vdw} : ligand–protein van der Waals interaction energy; E_{elect} : ligand–protein electrostatic interaction energy; $\Delta G_{gas} = E_{vdw} + E_{elect}$; E_{GB} : Generalized-Born electrostatic component of the solvation free energy; E_{SURF} : Solvent-accessible surface component of the solvation free energy; $\Delta G_{solv} = E_{GB} + E_{SURF}$; $\Delta G_{bind} = \Delta G_{gas} + \Delta G_{solv}$.

^aA total of 100 snapshots taken from the last 30 ns of the MD trajectories for the three simulated complexes were considered.

Table 6 Pharmacokinetic profile of **26**^a.

Subject	$t_{1/2}$ (h)	T_{max} (h)	C_{max} (ng/mL)	AUC_{0-last} (h·ng/mL)	AUC_{0-inf} (h·ng/mL)	CL (mL/min/kg)	F (%)
26 (i.v.) ^b	1.71 ± 0.24	—	941 ± 181	1290 ± 62.7	1336 ± 53.9	25.0 ± 1.04	—
26 (p.o.) ^c	2.68 ± 0.20	2.00 ± 0.32	762 ± 296	4359 ± 1570	4761 ± 1354	—	33.8

^aPK parameters (mean ± SD, $n = 3$).^bDosed i.v. at 2 mg/kg.^cDosed p.o. at 20 mg/kg —Not applicable.**Figure 6** The relative body weight changes of Kunming mice in different groups (**26** and blank).

Autosampler (Agilent, Palo Alto, CA, USA) was used to collect samples for measurement of mass spectra. All reactions were monitored by thin layer chromatography (TLC), and spots were visualized with iodine vapor or by irradiation with UV light. Flash column chromatography was performed on columns packed with silica gel (200–300 mesh, Qingdao, China). Solvents were of reagent grade and were purified by standard methods when necessary.

4.1.1. General procedure for the preparation of intermediates **6a–k**

4-Iodo-2,6-dimethylphenol (**5**, 1.00 mmol) and boric acid substituents (1.20 mmol) were dissolved in DMF (10 mL), then Pd(PPh₃)₄ (0.05 mmol) and 2 mol/L Na₂CO₃ aqueous solution (2.00 mmol) were added. The reaction mixture was stirred under N₂ at 100 °C for 6–10 h (monitored by TLC). The solution was cooled to room temperature and 10 mL of water was added. The aqueous layer was extracted with EtOAc, then the organic phase was dried over Na₂SO₄, filtered and evaporated under reduced pressure gave the intermediates **6a–k**, which were conducted next step without further purification.

4.1.2. General procedure for the preparation of intermediates **8a–k**

A reaction mixture of **6a–k** (10 mmol), 2,4-dichlorothiopheno [3,2-*d*]pyrimidine (2.1 g, 10 mmol) and potassium carbonate (1.7 g, 12 mmol) in DMF (30 mL) was stirred at room temperature for 2–4 h (monitoring with TLC), then the mixture was poured into water (100 mL). The precipitated white solid was collected by filtration, washed with water, and recrystallized in DMF-H₂O to provide the desired compounds **8a–k**.

4.1.2.1. 2-Chloro-4-(4-(furan-2-yl)-2,6-dimethylphenoxy)thieno [3,2-*d*]pyrimidine (**8a**). White solid, Yield 82%, m.p.:

175–177 °C. ¹H NMR (400 MHz, DMSO-*d*₆) δ 8.57 (d, $J = 5.4$ Hz, 1H, C6-thienopyrimidine-H), 7.78 (d, $J = 1.8$ Hz, 1H, C3-furan-H), 7.67 (d, $J = 5.4$ Hz, 1H, C7-thienopyrimidine-H), 7.57 (s, 2H, C₃,C₅-Ph'-H), 6.97 (d, $J = 3.3$ Hz, 1H, C5-furan-H), 6.63 (dd, $J = 3.4, 1.8$ Hz, 1H, C4-furan-H), 2.13 (s, 6H). ¹³C NMR (100 MHz, DMSO-*d*₆) δ 165.0, 163.7, 152.8, 148.3, 143.5, 140.3, 131.5, 129.1, 124.3, 124.1, 115.7, 112.6, 106.6, 16.4. ESI-MS: m/z 357.2 [M+H]⁺, 379.4 [M+Na]⁺. C₁₈H₁₃ClN₂O₂S (356.04).

4.1.2.2. 2-Chloro-4-(4-(furan-3-yl)-2,6-dimethylphenoxy)thieno [3,2-*d*]pyrimidine (**8b**). White solid, Yield 84%, m.p.: 163–165 °C. ¹H NMR (400 MHz, DMSO-*d*₆) δ 8.00 (d, $J = 5.3$ Hz, 1H, C6-thienopyrimidine-H), 7.57–7.56 (m, 2H), 7.52 (d, $J = 5.4$ Hz, 1H, C7-thienopyrimidine-H), 7.28 (s, 2H, C₃,C₅-Ph'-H), 7.13–7.12 (m, 1H), 2.20 (s, 6H). ¹³C NMR (100 MHz, DMSO-*d*₆) δ 164.5, 163.8, 163.7, 161.2, 156.8, 148.5, 138.5, 136.9, 136.6, 131.0, 128.7, 128.6, 127.5, 124.1, 115.7, 115.5, 16.6. ESI-MS: m/z 357.2 [M+H]⁺. C₁₈H₁₃ClN₂O₂S (356.04).

4.1.2.3. 2-Chloro-4-(2,6-dimethyl-4-(thiophen-2-yl)phenoxy)thieno[3,2-*d*]pyrimidine (**8c**). White solid, Yield 92%, m.p.: 143–145 °C. ¹H NMR (400 MHz, DMSO-*d*₆) δ 7.98 (d, $J = 5.4$ Hz, 1H, C6-thienopyrimidine-H), 7.50 (d, $J = 5.4$ Hz, 1H, C7-thienopyrimidine-H), 7.38 (s, 2H, C₃,C₅-Ph'-H), 7.31 (dd, $J = 3.6, 1.2$ Hz, 1H, C3-thiophen-H), 7.28 (dd, $J = 5.1, 1.1$ Hz, 1H, C5-thiophen-H), 7.08 (dd, $J = 5.1, 3.6$ Hz, 1H, C4-thiophen-H), 2.18 (s, 6H). ¹³C NMR (100 MHz, DMSO-*d*₆) δ 164.6, 163.8, 148.5, 143.5, 136.9, 132.7, 131.3, 128.0, 126.4, 124.9, 124.0, 123.3, 16.5. ESI-MS: m/z 373.2 [M+H]⁺. C₁₈H₁₃ClN₂OS₂ (372.02).

4.1.2.4. 2-Chloro-4-(2,6-dimethyl-4-(thiophen-3-yl)phenoxy)thieno[3,2-*d*]pyrimidine (**8d**). White solid, Yield 90%, m.p.: 140–142 °C. ¹H NMR (400 MHz, DMSO-*d*₆) δ 8.58 (d, $J = 5.3$ Hz, 1H, C6-thienopyrimidine-H), 7.91 (dd, $J = 3.0, 1.4$ Hz, 1H, C4-thiophen-H), 7.69–7.66 (m, 2H), 7.61 (d, $J = 1.4$ Hz, 1H, C5-thiophen-H), 7.59 (s, 2H, C₃,C₅-Ph'-H), 2.13 (s, 6H). ¹³C NMR (100 MHz, DMSO-*d*₆) δ 165.0, 163.7, 155.7, 148.1, 141.1, 140.2, 133.9, 131.2, 127.5, 127.0, 126.7, 124.1, 121.6, 115.8, 39.7, 16.5. ESI-MS: m/z 373.1 [M+H]⁺, 395.2 [M+Na]⁺. C₁₈H₁₃ClN₂OS₂ (372.02).

4.1.2.5. 2-Chloro-4-((3,5-dimethyl-[1,1'-biphenyl]-4-yl)oxy)thieno[3,2-*d*]pyrimidine (**8e**). White solid, Yield 93%, m.p.: 150–151 °C. ¹H NMR (400 MHz, DMSO-*d*₆) δ 8.59 (d, $J = 5.4$ Hz, 1H, C6-thienopyrimidine-H), 7.72 (d, $J = 7.3$ Hz, 2H, C₂,C₆-Ph''-H), 7.68 (d, $J = 5.4$ Hz, 1H, C7-thienopyrimidine-H), 7.53 (s, 2H, C₃,C₅-Ph'-H), 7.49 (t, $J = 7.5$ Hz, 2H, C₃,C₅-

Ph''-H), 7.40 (d, $J = 7.5$ Hz, 1H, C4-Ph''-H), 2.16 (s, 6H). ^{13}C NMR (100 MHz, DMSO- d_6) δ 165.0, 164.9, 163.7, 163.3, 155.7, 148.6, 140.3, 139.8, 138.8, 137.7, 133.6, 131.2, 129.3, 127.9, 127.2, 124.1, 115.9, 92.2, 16.5. ESI-MS: m/z 367.2 [M+H] $^+$, 389.2 [M+Na] $^+$. C₂₀H₁₅CIN₂OS (366.06).

4.1.2.6. 2-Chloro-4-((4'-methoxy-3,5-dimethyl-[1,1'-biphenyl]-4-yl)oxy)thieno[3,2-*d*]pyrimidine (**8f**). White solid, Yield 94%, m.p.: 150–151 °C. ^1H NMR (400 MHz, DMSO- d_6) δ 7.97 (d, $J = 5.4$ Hz, 1H, C6-thienopyrimidine-H), 7.52 (s, 2H, C2, C6-Ph''-H), 7.50 (d, $J = 5.6$ Hz, 1H, C7-thienopyrimidine-H), 7.30 (s, 2H, C3, C5-Ph'-H), 6.99–6.91 (m, 2H, C3, C5-Ph''-H), 3.85 (s, 3H, CH₃), 2.19 (s, 6H). ^{13}C NMR (100 MHz, DMSO- d_6) δ 164.5, 163.9, 159.2, 148.1, 139.1, 136.9, 132.9, 130.9, 128.1, 127.2, 124.0, 114.1, 55.3, 16.6. ESI-MS: m/z 397.2 [M+H] $^+$, 419.2 [M+Na] $^+$. C₂₁H₁₇CIN₂O₂S (396.07).

4.1.2.7. 2-Chloro-4-((4'-fluoro-3,5-dimethyl-[1,1'-biphenyl]-4-yl)oxy)thieno[3,2-*d*]pyrimidine (**8g**). White solid, Yield 89%, m.p.: 126–128 °C. ^1H NMR (400 MHz, DMSO- d_6) δ 7.98 (d, $J = 5.4$ Hz, 1H, C6-thienopyrimidine-H), 7.74–7.68 (m, 2H, C2, C6-Ph''-H), 7.51 (d, $J = 5.6$ Hz, 1H, C7-thienopyrimidine-H), 7.31 (s, 2H, C3, C5-Ph'-H), 6.72–6.70 (m, 2H, C3, C5-Ph''-H), 2.17 (s, 6H). ^{13}C NMR (100 MHz, DMSO- d_6) δ 164.5, 163.8, 156.8, 148.0, 143.7, 138.5, 136.9, 131.1, 130.7, 127.6, 126.3, 125.7, 124.0, 115.4, 108.9, 16.5. ESI-MS: m/z 385.2 [M+H] $^+$, 407.3 [M+Na] $^+$. C₂₀H₁₄ClF₂OS (384.05).

4.1.2.8. 4'-((2-Chlorothieno[3,2-*d*]pyrimidin-4-yl)oxy)-3',5'-dimethyl-[1,1'-biphenyl]-4-carbonitrile (**8h**). White solid, Yield 85%, m.p.: 131–133 °C. ^1H NMR (400 MHz, DMSO- d_6) δ 8.59 (d, $J = 5.4$ Hz, 1H, C6-thienopyrimidine-H), 7.95 (s, 4H, Ph''-H), 7.68 (d, $J = 5.4$ Hz, 1H, C7-thienopyrimidine-H), 7.64 (s, 2H, C3, C5-Ph'-H), 2.16 (s, 6H). ^{13}C NMR (100 MHz, DMSO- d_6) δ 165.0, 163.6, 149.6, 144.2, 140.3, 136.8, 133.2, 131.6, 128.1, 128.0, 124.2, 119.3, 110.5, 16.5. ESI-MS: m/z 392.2 [M+H] $^+$, C₂₁H₁₄CIN₃OS (391.05).

4.1.2.9. 4'-((2-Chlorothieno[3,2-*d*]pyrimidin-4-yl)oxy)-3',5'-dimethyl-[1,1'-biphenyl]-3-carbonitrile (**8i**). White solid, Yield 82%, m.p.: 142–144 °C. ^1H NMR (400 MHz, DMSO- d_6) δ 8.03 (d, $J = 5.4$ Hz, 1H, C6-thienopyrimidine-H), 7.86 (t, $J = 1.7$ Hz, 1H, C4-Ph''-H), 7.82 (dt, $J = 7.9, 1.6$ Hz, 1H, C6-Ph''-H), 7.66–7.62 (m, 1H, C2-Ph''-H), 7.56 (d, $J = 7.8$ Hz, 1H, C5-Ph''-H), 7.53 (d, $J = 5.4$ Hz, 1H, C7-thienopyrimidine-H), 7.31 (s, 2H, C3, C5-Ph'-H), 2.22 (s, 6H). ^{13}C NMR (100 MHz, DMSO- d_6) δ 164.6, 163.6, 149.3, 141.7, 137.0, 136.9, 131.5, 131.4, 130.7, 129.5, 127.6, 124.1, 118.8, 112.9, 16.6. ESI-MS: m/z 392.2 [M+H] $^+$, 414.2 [M+Na] $^+$. C₂₁H₁₄CIN₃OS (391.05).

4.1.2.10. 4'-((2-Chlorothieno[3,2-*d*]pyrimidin-4-yl)oxy)-*N,N,N',N'*-tetramethyl-[1,1'-biphenyl]-4-amine (**8j**). White solid, Yield 88%, m.p.: 137–138 °C. ^1H NMR (400 MHz, DMSO- d_6) δ 7.95 (d, $J = 5.5$ Hz, 1H, C6-thienopyrimidine-H), 7.51 (d, $J = 8.9$ Hz, 2H, C2, C6-Ph''-H), 7.49 (d, $J = 5.6$ Hz, 1H, C7-thienopyrimidine-H), 7.30 (s, 2H, C3, C5-Ph'-H), 6.81 (d, $J = 8.8$ Hz, 2H, C3, C5-Ph''-H), 3.00 (s, 6H, NCH₃), 2.18 (s, 6H). ^{13}C NMR (100 MHz, DMSO- d_6) δ 164.6, 164.0, 156.8, 150.0,

147.6, 139.5, 136.9, 130.8, 128.3, 127.6, 126.7, 124.0, 115.4, 112.7, 76.8, 40.6, 16.7. ESI-MS: m/z 410.2 [M+H] $^+$. C₂₂H₂₀CIN₃OS (409.10).

4.1.2.11. 4'-((2-Chlorothieno[3,2-*d*]pyrimidin-4-yl)oxy)-*N,N,N',N'*-tetramethyl-[1,1'-biphenyl]-3-amine (**8k**). White solid, Yield 84%, m.p.: 130–132 °C. ^1H NMR (400 MHz, DMSO- d_6) δ 7.98 (d, $J = 5.5$ Hz, 1H, C6-thienopyrimidine-H), 7.51 (d, $J = 5.4$ Hz, 1H, C7-thienopyrimidine-H), 7.34 (s, 2H, C3, C5-Ph'-H), 7.32–7.24 (m, 1H), 6.99–6.91 (m, 2H), 6.75 (dd, $J = 8.3, 2.5$ Hz, 1H, C5-Ph''-H), 3.03 (s, 6H, NCH₃), 2.20 (s, 6H). ^{13}C NMR (100 MHz, DMSO- d_6) δ 164.5, 163.9, 156.8, 150.9, 148.4, 141.4, 140.6, 136.9, 130.8, 129.4, 127.8, 124.0, 115.8, 115.5, 111.7, 111.5, 40.7, 16.6. ESI-MS: m/z 410.2 [M+H] $^+$, 422.2 [M+Na] $^+$. C₂₂H₂₀CIN₃OS (409.10).

4.1.3. General procedure for the preparation of intermediates **10a–k**

PdCl₂(PPh₃)₂ (0.07 g, 0.1 mmol) and BINAP (0.06 g, 0.1 mmol) were dissolved in dry dioxane (20 mL), and then *tert*-butyl(4-aminophenyl)carbamate (0.50 g, 2.4 mmol), intermediates **8a–k** (0.01 mmol) and Cs₂CO₃ (0.97 g, 3.0 mmol) were added to the solution. The reaction mixture was stirred under N₂ at 120 °C for 10–12 h (monitoring with TLC). After cooling to room temperature, the solvent was evaporated under reduce pressure, and EtOAc was added to the residue. The organic layer was extracted three times with water, then the organic phase was dried over Na₂SO₄, filtered and evaporated under reduced pressure gave the intermediates **9a–k**, which was used directly in the next step without further purification. Then the intermediates **9a–k** (2.0 mmol) and TFA (1.50 mL, 20 mmol) were dissolved in DCM (4 mL), the mixed solution was stirred for 3–6 h (monitored by TLC) at room temperature. Then the solution was alkalized to pH 9 with saturated NaHCO₃ and extracted with DCM (3 × 5 mL). The organic phase was dried over anhydrous Na₂SO₄, filtered, concentrated and purified by flash column chromatography to give the intermediates **10a–k**.

4.1.3.1. 4-(4-(Furan-2-yl)-2,6-dimethylphenoxy)-*N*-(piperidin-4-yl)thieno[3,2-*d*]pyrimidin-2-amine (**10a**). White solid, Yield 56%, m.p.: 150–152 °C. ^1H NMR (400 MHz, chloroform-*d*) δ 9.20 (s, 1H, NH), 7.78 (d, $J = 5.4$ Hz, 1H, C6-thienopyrimidine-H), 7.45 (d, $J = 1.7$ Hz, 1H, C3-furan-H), 7.42 (s, 2H, C3, C5-Ph'-H), 7.21 (d, $J = 5.4$ Hz, 1H, C7-thienopyrimidine-H), 6.62 (d, $J = 3.3$ Hz, 1H, C5-furan-H), 6.46 (dd, $J = 3.4, 1.8$ Hz, 1H, C4-furan-H), 5.25 (s, 1H, NH), 3.87 (s, 1H), 3.33–3.30 (m, 2H), 2.87 (s, 2H), 2.16 (s, 6H), 2.11–2.02 (m, 2H), 1.75–1.67 (s, 2H). ^{13}C NMR (100 MHz, chloroform-*d*) δ 163.7, 159.6, 153.3, 148.7, 142.1, 135.2, 131.4, 128.7, 123.9, 122.9, 111.7, 107.4, 105.0, 46.3, 42.7, 28.5, 16.5. ESI-MS: m/z 421.2 [M+H] $^+$. C₂₃H₂₄N₄O₂S (420.16).

4.1.3.2. 4-(4-(Furan-3-yl)-2,6-dimethylphenoxy)-*N*-(piperidin-4-yl)thieno[3,2-*d*]pyrimidin-2-amine (**10b**). White solid, Yield 50%, m.p.: 148–150 °C. ^1H NMR (400 MHz, chloroform-*d*) δ 8.23 (d, $J = 5.4$ Hz, 1H, C6-thienopyrimidine-H), 7.92–7.91 (m, 2H), 7.83 (d, $J = 5.4$ Hz, 1H, C7-thienopyrimidine-H), 7.46 (s, 2H, C3, C5-Ph'-H), 7.42–7.41 (m, 1H), 5.32 (s, 1H, NH), 3.88

(s, 1H), 3.30–3.27 (m, 2H), 2.87–2.85 (m, 2H), 2.21 (s, 6H), 2.03–1.71 (m, 4H). ^{13}C NMR (100 MHz, chloroform-*d*) δ 165.2, 164.7, 163.9, 161.5, 155.9, 147.6, 138.7, 136.1, 135.7, 131.6, 128.7, 126.8, 124.9, 115.7, 115.2, 46.4, 42.2, 28.7, 16.6. ESI-MS: m/z 421.2 $[\text{M}+\text{H}]^+$, 438.3 $[\text{M}+\text{NH}_4]^+$. $\text{C}_{23}\text{H}_{24}\text{N}_4\text{O}_2\text{S}$ (420.16).

4.1.3.3. 4-(2,6-Dimethyl-4-(thiophen-2-yl)phenoxy)-*N*-(piperidin-4-yl)thieno[3,2-*d*]pyrimidin-2-amine (**10c**). White solid, Yield 47%, m.p.: 161–162 °C. ^1H NMR (400 MHz, chloroform-*d*) δ 7.92 (d, $J = 5.3$ Hz, 1H, C6-thienopyrimidine-H), 7.48 (d, $J = 5.4$ Hz, 1H, C7-thienopyrimidine-H), 7.32 (s, 2H, C3,C5-Ph'-H), 7.31 (dd, $J = 3.6, 1.1$ Hz, 1H, C3-thiophen-H), 7.27 (dd, $J = 5.2, 1.1$ Hz, 1H, C5-thiophen-H), 7.10 (dd, $J = 5.2, 3.6$ Hz, 1H, C4-thiophen-H), 5.32 (s, 1H, NH), 3.88 (s, 1H), 3.30–3.27 (m, 2H), 2.86–2.85 (m, 2H), 2.18 (s, 6H), 2.03–1.71 (m, 4H). ^{13}C NMR (100 MHz, chloroform-*d*) δ 164.6, 163.8, 148.5, 143.5, 136.9, 132.7, 131.3, 128.0, 126.4, 124.9, 124.0, 123.3, 46.3, 42.5, 28.6, 16.5. ESI-MS: m/z 437.2 $[\text{M}+\text{H}]^+$. $\text{C}_{23}\text{H}_{24}\text{N}_4\text{OS}_2$ (436.14).

4.1.3.4. 4-(2,6-Dimethyl-4-(thiophen-3-yl)phenoxy)-*N*-(piperidin-4-yl)thieno[3,2-*d*]pyrimidin-2-amine (**10d**). White solid, Yield 57%, m.p.: 157–159 °C. ^1H NMR (400 MHz, chloroform-*d*) δ 8.52 (d, $J = 5.4$ Hz, 1H, C6-thienopyrimidine-H), 7.87 (dd, $J = 3.1, 1.5$ Hz, 1H, C4-thiophen-H), 7.68–7.62 (m, 2H), 7.61 (d, $J = 1.5$ Hz, 1H, C5-thiophen-H), 7.58 (s, 2H, C3,C5-Ph'-H), 5.31 (s, 1H, NH), 3.88 (s, 1H), 3.29–3.28 (m, 2H), 2.86–2.83 (m, 2H), 2.13 (s, 6H), 2.01–1.98 (m, 2H), 1.74–1.52 (m, 2H). ^{13}C NMR (100 MHz, chloroform-*d*) δ 165.2, 163.5, 155.9, 148.6, 143.6, 141.3, 140.0, 133.4, 131.2, 127.8, 127.0, 126.4, 123.9, 121.6, 116.0, 46.3, 39.7, 28.6, 16.5. ESI-MS: m/z 437.2 $[\text{M}+\text{H}]^+$, 454.6 $[\text{M}+\text{NH}_4]^+$. $\text{C}_{23}\text{H}_{24}\text{N}_4\text{OS}_2$ (436.14).

4.1.3.5. 4-((3,5-Dimethyl-[1,1'-biphenyl]-4-yl)oxy)-*N*-(piperidin-4-yl)thieno[3,2-*d*]pyrimidin-2-amine (**10e**). White solid, Yield 46%, m.p.: 153–155 °C. ^1H NMR (400 MHz, chloroform-*d*) δ 7.79 (d, $J = 5.4$ Hz, 1H, C6-thienopyrimidine-H), 7.59 (d, $J = 7.2$ Hz, 2H, C2,C6-Ph''-H), 7.43 (t, $J = 7.6$ Hz, 2H, C3,C5-Ph'-H), 7.34–7.32 (m, 3H), 7.21 (d, $J = 5.4$ Hz, 1H, C7-thienopyrimidine-H), 5.04 (s, 1H, NH), 3.89 (s, 1H), 3.32–3.30 (m, 2H), 2.92–2.87 (m, 2H), 2.20 (s, 6H), 2.16–2.05 (m, 2H), 1.77–1.69 (m, 2H). ^{13}C NMR (100 MHz, chloroform-*d*) δ 177.8, 167.9, 163.6, 159.8, 155.2, 149.0, 144.4, 140.4, 139.0, 135.0, 132.1, 131.3, 128.7, 127.0, 123.1, 115.0, 107.5, 46.3, 42.7, 28.6, 16.6. ESI-MS: m/z 431.3 $[\text{M}+\text{H}]^+$, 453.4 $[\text{M}+\text{Na}]^+$. $\text{C}_{25}\text{H}_{26}\text{N}_4\text{OS}$ (430.18).

4.1.3.6. 4-((4'-Methoxy-3,5-dimethyl-[1,1'-biphenyl]-4-yl)oxy)-*N*-(piperidin-4-yl)thieno[3,2-*d*]pyrimidin-2-amine (**10f**). White solid, Yield 67%, m.p.: 158–160 °C. ^1H NMR (400 MHz, chloroform-*d*) δ 7.77 (d, $J = 5.4$ Hz, 1H, C6-thienopyrimidine-H), 7.54–7.47 (m, 2H, C2,C6-Ph''-H), 7.27 (s, 2H, C3,C5-Ph'-H), 7.21 (d, $J = 5.4$ Hz, 1H, C7-thienopyrimidine-H), 6.96 (d, $J = 2.7$ Hz, 2H), 5.01 (s, 1H, NH), 3.84 (s, 1H), 3.83 (s, 3H), 3.32–3.31 (m, 2H), 2.95–2.87 (m, 2H), 2.18 (s, 6H), 2.12–2.04 (m, 4H). ^{13}C NMR (100 MHz, chloroform-*d*) δ 164.7, 163.6, 159.8, 159.1, 148.5, 138.6, 135.0, 133.0, 131.2, 128.0, 127.3, 126.8, 123.1, 114.2, 55.3, 42.8, 28.5, 16.6. ESI-MS: m/z 461.3 $[\text{M}+\text{H}]^+$, 478.2 $[\text{M}+\text{NH}_4]^+$. $\text{C}_{26}\text{H}_{28}\text{N}_4\text{O}_2\text{S}$ (460.19).

4.1.3.7. 4-((4'-Fluoro-3,5-dimethyl-[1,1'-biphenyl]-4-yl)oxy)-*N*-(piperidin-4-yl)thieno[3,2-*d*]pyrimidin-2-amine (**10g**). White

solid, Yield 48%, m.p.: 145–147 °C. ^1H NMR (400 MHz, chloroform-*d*) δ 7.84 (d, $J = 5.4$ Hz, 1H, C6-thienopyrimidine-H), 7.72–7.66 (m, 2H, C2,C6-Ph''-H), 7.43 (d, $J = 5.4$ Hz, 1H, C7-thienopyrimidine-H), 7.32 (s, 2H, C3,C5-Ph'-H), 6.71–6.68 (m, 2H, C3,C5-Ph''-H), 5.03 (s, 1H, NH), 3.86 (s, 1H), 3.30 (s, 2H), 2.90–2.86 (m, 2H), 2.17 (s, 6H), 2.12–1.45 (m, 4H). ^{13}C NMR (100 MHz, chloroform-*d*) δ 167.8, 164.3, 163.4, 156.8, 148.2, 143.7, 138.7, 137.0, 130.7, 130.1, 127.6, 126.0, 125.7, 124.0, 115.1, 109.0, 46.5, 42.3, 28.2, 16.4. ESI-MS: m/z 449.2 $[\text{M}+\text{H}]^+$, 471.3 $[\text{M}+\text{Na}]^+$. $\text{C}_{25}\text{H}_{25}\text{FN}_4\text{OS}$ (448.17).

4.1.3.8. 3',5'-Dimethyl-4'-((2-(piperidin-4-ylamino)thieno[3,2-*d*]pyrimidin-4-yl)oxy)-[1,1'-biphenyl]-4-carbonitrile (**10h**). White solid, Yield 60%, m.p.: 157–159 °C. ^1H NMR (400 MHz, chloroform-*d*) δ 8.52 (d, $J = 5.4$ Hz, 1H, C6-thienopyrimidine-H), 7.95–7.92 (m, 4H), 7.65 (d, $J = 5.3$ Hz, 1H, C7-thienopyrimidine-H), 7.62 (s, 2H, C3,C5-Ph'-H), 5.02 (s, 1H, NH), 3.85 (s, 1H), 3.30–3.19 (m, 2H), 2.89–2.85 (m, 2H), 2.16 (s, 6H), 2.09–1.32 (m, 4H). ^{13}C NMR (100 MHz, chloroform-*d*) δ 172.3, 167.3, 165.1, 163.2, 150.7, 144.1, 139.2, 137.0, 133.0, 131.2, 128.4, 128.0, 124.5, 120.5, 110.7, 46.6, 42.4, 28.1, 16.5. ESI-MS: m/z 456.2 $[\text{M}+\text{H}]^+$, 473.4 $[\text{M}+\text{NH}_4]^+$. $\text{C}_{26}\text{H}_{25}\text{N}_5\text{OS}$ (455.18).

4.1.3.9. 3',5'-Dimethyl-4'-((2-(piperidin-4-ylamino)thieno[3,2-*d*]pyrimidin-4-yl)oxy)-[1,1'-biphenyl]-3-carbonitrile (**10i**). White solid, Yield 55%, m.p.: 171–173 °C. ^1H NMR (400 MHz, chloroform-*d*) δ 8.06 (d, $J = 5.3$ Hz, 1H, C6-thienopyrimidine-H), 7.89–7.88 (m, 1H, C4-Ph''-H), 7.84 (dt, $J = 7.8, 1.6$ Hz, 1H, C6-Ph''-H), 7.69–7.64 (m, 1H, C2-Ph''-H), 7.57 (d, $J = 7.8$ Hz, 1H, C5-Ph''-H), 7.52 (d, $J = 5.4$ Hz, 1H, C7-thienopyrimidine-H), 7.30 (s, 2H, C3,C5-Ph'-H), 5.01 (s, 1H, NH), 3.86 (s, 1H), 3.30–3.19 (m, 2H), 2.88–2.85 (m, 2H), 2.18 (s, 6H), 2.03–1.88 (m, 2H), 1.67–1.51 (m, 2H). ^{13}C NMR (100 MHz, chloroform-*d*) δ 167.3, 164.2, 162.7, 149.03, 141.4, 137.4, 137.0, 131.9, 131.4, 130.8, 129.9, 126.8, 124.4, 119.3, 113.2, 46.4, 42.1, 28.5, 16.6. ESI-MS: m/z 456.2 $[\text{M}+\text{H}]^+$, 473.6 $[\text{M}+\text{NH}_4]^+$. $\text{C}_{26}\text{H}_{25}\text{N}_5\text{OS}$ (455.18).

4.1.3.10. 4-((4'-(Dimethylamino)-3,5-dimethyl-[1,1'-biphenyl]-4-yl)oxy)-*N*-(piperidin-4-yl)thieno[3,2-*d*]pyrimidin-2-amine (**10j**). White solid, Yield 63%, m.p.: 170–171 °C. ^1H NMR (400 MHz, chloroform-*d*) δ 7.98 (d, $J = 5.3$ Hz, 1H, C6-thienopyrimidine-H), 7.52 (d, $J = 8.6$ Hz, 2H, C2,C6-Ph''-H), 7.51 (d, $J = 5.4$ Hz, 1H, C7-thienopyrimidine-H), 7.32 (s, 2H, C3,C5-Ph'-H), 6.82 (d, $J = 8.8$ Hz, 2H, C3,C5-Ph''-H), 5.01 (s, 1H, NH), 3.84 (s, 1H), 3.33–3.31 (m, 2H), 3.02 (s, 6H, NCH₃), 2.18 (s, 6H), 2.09–1.61 (m, 6H). ^{13}C NMR (100 MHz, chloroform-*d*) δ 167.2, 164.3, 163.8, 156.0, 150.3, 147.1, 140.8, 136.2, 130.6, 128.3, 127.2, 126.7, 124.7, 115.4, 112.8, 46.3, 42.7, 40.6, 28.4, 16.7. ESI-MS: m/z 474.2 $[\text{M}+\text{H}]^+$, 491.2 $[\text{M}+\text{NH}_4]^+$. $\text{C}_{27}\text{H}_{31}\text{N}_5\text{OS}$ (473.22).

4.1.3.11. 4-((3'-(Dimethylamino)-3,5-dimethyl-[1,1'-biphenyl]-4-yl)oxy)-*N*-(piperidin-4-yl)thieno[3,2-*d*]pyrimidin-2-amine (**10k**). White solid, Yield 50%, m.p.: 166–167 °C. ^1H NMR (400 MHz, chloroform-*d*) δ 7.83 (d, $J = 5.3$ Hz, 1H, C6-thienopyrimidine-H), 7.50 (d, $J = 5.3$ Hz, 1H, C7-thienopyrimidine-H), 7.32 (s, 2H, C3,C5-Ph'-H), 7.31–7.25 (m, 1H), 6.98–6.92 (m, 2H), 6.72 (dd, $J = 8.8, 2.4$ Hz, 1H, C5-Ph''-H), 5.00 (s, 1H, NH), 3.83 (s, 1H), 3.32–3.30 (m, 2H), 3.03 (s, 6H, NCH₃), 2.86–1.83 (m, 2H), 2.20 (s, 6H), 2.12–1.54 (m, 4H). ^{13}C

NMR (100 MHz, chloroform-*d*) δ 167.6, 164.2, 163.5, 156.4, 150.5, 148.6, 141.3, 139.6, 136.2, 130.8, 129.8, 127.1, 124.0, 115.7, 115.5, 112.0, 111.2, 46.5, 42.4, 40.6, 28.3, 16.6. ESI-MS: m/z 474.3 [M+H]⁺, 491.2 [M+NH₄]⁺. C₂₇H₃₁N₅O₅ (473.22).

4.1.4. General procedure for the preparation of the target compounds **11–32**

Compounds **10a–k** (1.0 mmol), substituted benzyl chloride (bromine) (1.1 mmol) and anhydrous K₂CO₃ (1.2 mmol) were dissolved in anhydrous DMF (10 mL). The reaction mixture was stirred at room temperature for 4–8 h (monitored by TLC). The solvent was removed under reduced pressure, and then water was added. Extracted with ethyl acetate (3 × 10 mL), and the organic phase was dried over anhydrous Na₂SO₄, then purified by flash column chromatography and recrystallized from EA/PE to give the target compounds **11–32**.

4.1.4.1. 4-((4-((4-(4-(Furan-2-yl)-2,6-dimethylphenoxy)thieno[3,2-*d*]pyrimidin-2-yl)amino)piperidin-1-yl)methyl)benzenesulfonamide (**11**). White solid, Yield 77%, m.p.: 158–160 °C. ¹H NMR (400 MHz, chloroform-*d*) δ 7.83 (d, *J* = 8.0 Hz, 2H, C2,C6-Ph''-H), 7.72 (d, *J* = 5.4 Hz, 1H, C6-thienopyrimidine-H), 7.48 (d, *J* = 1.7 Hz, 1H, C3-furan-H), 7.40 (s, 4H), 7.15 (d, *J* = 5.4 Hz, 1H, C7-thienopyrimidine-H), 6.62 (d, *J* = 3.3 Hz, 1H, C5-furan-H), 6.49 (dd, *J* = 3.4, 1.8 Hz, C4-furan-H), 5.44–5.24 (m, 2H, SO₂NH₂), 5.16 (s, 1H, NH), 3.47 (s, 2H, N-CH₂), 2.69–2.65 (m, 2H), 2.15 (s, 6H), 2.07–1.21 (m, 7H). ¹³C NMR (100 MHz, chloroform-*d*) δ 165.0, 163.5, 160.3, 153.6, 149.0, 143.9, 142.0, 140.7, 134.8, 131.6, 129.5, 128.5, 126.3, 123.9, 123.0, 111.7, 104.8, 62.3, 52.1, 48.3, 31.8, 16.6. HRMS m/z C₃₀H₃₁N₅O₄S₂: Calcd. 589.1817, Found 590.1895 [M+H]⁺. HPLC purity: 96.83%.

4.1.4.2. 4-((4-((4-(4-(Furan-2-yl)-2,6-dimethylphenoxy)thieno[3,2-*d*]pyrimidin-2-yl)amino)piperidin-1-yl)methyl)benzamide (**12**). White solid, Yield 79%, m.p.: 167–168 °C. ¹H NMR (400 MHz, chloroform-*d*) δ 7.84 (d, *J* = 8.1 Hz, 2H, C2,C6-Ph''-H), 7.72 (d, *J* = 5.3 Hz, 1H, C6-thienopyrimidine-H), 7.46 (d, *J* = 1.7 Hz, 1H, C3-furan-H), 7.42–7.40 (m, 4H), 7.15 (d, *J* = 5.3 Hz, 1H, C7-thienopyrimidine-H), 6.62 (d, *J* = 3.2 Hz, 1H, C5-furan-H), 6.48 (dd, *J* = 3.2, 1.8 Hz, C4-furan-H), 6.07–5.88 (m, 2H, CONH₂), 5.16 (s, 1H, NH), 3.47 (s, 2H, N-CH₂), 2.69–2.65 (m, 2H), 2.15 (s, 6H), 2.07–1.21 (m, 7H). ¹³C NMR (100 MHz, chloroform-*d*) δ 165.1, 163.5, 160.2, 153.6, 149.1, 143.7, 142.2, 140.9, 134.4, 131.6, 129.7, 128.5, 126.3, 123.0, 114.3, 111.7, 104.7, 62.4, 52.1, 48.3, 31.8, 16.6. HRMS m/z C₃₁H₃₁N₅O₃S: Calcd. 553.2148, Found 554.2225 [M+H]⁺. HPLC purity: 97.63%.

4.1.4.3. 4-((4-((4-(4-(Furan-3-yl)-2,6-dimethylphenoxy)thieno[3,2-*d*]pyrimidin-2-yl)amino)piperidin-1-yl)methyl)benzenesulfonamide (**13**). White solid, Yield 81%, m.p.: 154–156 °C. ¹H NMR (400 MHz, chloroform-*d*) δ 7.83 (d, *J* = 8.1 Hz, 2H), 7.74 (d, *J* = 5.4 Hz, 1H, C6-thienopyrimidine-H), 7.56 (d, *J* = 5.4 Hz, 1H), 7.53 (d, *J* = 5.3 Hz, 1H, C7-thienopyrimidine-H), 7.40 (d, *J* = 8.0 Hz, 2H), 7.16 (d, *J* = 7.1 Hz, 1H), 7.12 (d, *J* = 8.6 Hz, 1H), 5.23 (s, 2H, SO₂NH₂), 5.00 (s, 1H, NH), 3.47 (s, 2H, N-CH₂), 2.70 (d, *J* = 10.9 Hz, 2H), 2.18 (s, 6H), 2.11–1.33 (m, 7H). ¹³C NMR (100 MHz, chloroform-*d*) δ 165.0, 160.4, 149.1, 144.1, 140.6, 137.7, 136.8, 134.7, 131.5, 129.4, 128.6, 127.0,

126.3, 123.0, 115.7, 62.3, 52.3, 31.9, 16.6. HRMS m/z C₃₀H₃₁N₅O₄S₂: Calcd. 589.1817, Found 590.1886 [M+H]⁺. HPLC purity: 97.30%.

4.1.4.4. 4-((4-((4-(4-(Furan-3-yl)-2,6-dimethylphenoxy)thieno[3,2-*d*]pyrimidin-2-yl)amino)piperidin-1-yl)methyl)benzamide (**14**). White solid, Yield 83%, m.p.: 182–185 °C. ¹H NMR (400 MHz, chloroform-*d*) δ 7.74 (t, *J* = 2.7 Hz, 2H), 7.72 (s, 1H), 7.56–7.54 (m, 2H), 7.34 (d, *J* = 7.8 Hz, 2H), 7.27 (d, *J* = 2.1 Hz, 2H), 7.19 (d, *J* = 5.4 Hz, 1H), 7.13 (t, *J* = 8.6 Hz, 1H), 6.08–5.82 (m, 2H, CONH₂), 4.93 (d, *J* = 8.0 Hz, 1H, NH), 3.47 (s, 2H, N-CH₂), 2.72 (d, *J* = 11.3 Hz, 2H), 2.19 (s, 6H), 2.07–1.84 (m, 7H). ¹³C NMR (100 MHz, chloroform-*d*) δ 169.2, 165.1, 161.2, 160.4, 149.2, 143.0, 137.7, 136.8, 134.6, 132.0, 131.5, 129.1, 128.6, 128.5, 127.3, 127.0, 123.2, 115.7, 115.4, 62.6, 52.3, 32.0, 16.6. HRMS m/z C₃₁H₃₁N₅O₃S: Calcd. 553.2148, Found 554.22195 [M+H]⁺. HPLC purity: 98.82%.

4.1.4.5. 4-((4-((4-(2,6-Dimethyl-4-(thiophen-2-yl)phenoxy)thieno[3,2-*d*]pyrimidin-2-yl)amino)piperidin-1-yl)methyl)benzenesulfonamide (**15**). White solid, Yield 69%, m.p.: 138–140 °C. ¹H NMR (400 MHz, chloroform-*d*) δ 7.95 (d, *J* = 8.2 Hz, 2H, C2,C6-Ph''-H), 7.76 (d, *J* = 5.3 Hz, 1H, C6-thienopyrimidine-H), 7.42–7.40 (m, 4H), 7.32 (dd, *J* = 3.5, 1.2 Hz, 1H, C3-thiophen-H), 7.29 (dd, *J* = 5.2, 1.2 Hz, 1H, C5-thiophen-H), 7.19 (d, *J* = 5.3 Hz, 1H, C7-thienopyrimidine-H), 7.03 (dd, *J* = 5.2, 3.6 Hz, 1H, C4-thiophen-H), 5.41–5.30 (m, 2H, SO₂NH₂), 5.11 (s, 1H, NH), 3.47 (s, 2H, N-CH₂), 2.69–2.65 (m, 2H), 2.12 (s, 6H), 2.01–1.43 (m, 7H). ¹³C NMR (100 MHz, chloroform-*d*) δ 165.2, 163.8, 160.4, 153.6, 149.2, 143.5, 142.4, 140.7, 134.2, 131.6, 130.2, 128.7, 126.3, 123.9, 123.1, 111.7, 104.2, 52.1, 48.3, 31.8, 28.6, 16.6. HRMS m/z C₃₀H₃₁N₅O₃S₃: Calcd. 605.1589, Found 606.1656 [M+H]⁺. HPLC purity: 92.90%.

4.1.4.6. 4-((4-((4-(2,6-Dimethyl-4-(thiophen-2-yl)phenoxy)thieno[3,2-*d*]pyrimidin-2-yl)amino)piperidin-1-yl)methyl)benzamide (**16**). White solid, Yield 78%, m.p.: 148–150 °C. ¹H NMR (400 MHz, chloroform-*d*) δ 7.92 (d, *J* = 8.2 Hz, 2H, C2,C6-Ph''-H), 7.79 (d, *J* = 5.4 Hz, 1H, C6-thienopyrimidine-H), 7.40–7.38 (m, 4H), 7.31 (dd, *J* = 3.5, 1.2 Hz, 1H, C3-thiophen-H), 7.29–7.28 (m, 1H), 7.19 (d, *J* = 5.4 Hz, 1H, C7-thienopyrimidine-H), 7.07 (dd, *J* = 5.1, 3.4 Hz, 1H, C4-thiophen-H), 6.03 (s, 2H, CONH₂), 5.10 (s, 1H, NH), 3.48 (s, 2H, N-CH₂), 2.70–2.68 (m, 2H), 2.11 (s, 6H), 1.98–1.40 (m, 7H). ¹³C NMR (100 MHz, chloroform-*d*) δ 165.3, 163.2, 160.8, 152.9, 148.7, 143.1, 142.7, 140.7, 134.6, 131.2, 130.2, 128.4, 126.3, 124.0, 123.1, 111.2, 104.2, 52.1, 48.5, 31.8, 28.2, 16.6. HRMS m/z C₃₁H₃₁N₅O₂S₂: Calcd. 569.1919, Found 570.1987 [M+H]⁺. HPLC purity: 99.90%.

4.1.4.7. 4-((4-((4-(2,6-Dimethyl-4-(thiophen-3-yl)phenoxy)thieno[3,2-*d*]pyrimidin-2-yl)amino)piperidin-1-yl)methyl)benzenesulfonamide (**17**). White solid, Yield 86%, m.p.: 168–170 °C. ¹H NMR (400 MHz, chloroform-*d*) δ 7.83 (d, *J* = 8.0 Hz, 2H, C2,C6-Ph''-H), 7.73 (d, *J* = 5.4 Hz, 1H, C6-thienopyrimidine-H), 7.43 (d, *J* = 1.6 Hz, 1H), 7.41–7.36 (m, 4H), 7.31 (s, 2H, C3,C5-Ph'-H), 7.16 (d, *J* = 5.4 Hz, 1H, C7-thienopyrimidine-H), 5.16 (s, 2H, SO₂NH₂), 5.00 (s, 1H, NH), 3.46 (s, 2H, N-CH₂), 2.69 (d, *J* = 11.2 Hz, 2H), 2.17 (s, 6H), 2.07–1.59 (m, 7H). ¹³C NMR (100 MHz, chloroform-*d*) δ 165.0, 163.5, 160.4, 148.9, 144.1,

141.8, 140.6, 134.7, 133.4, 131.5, 129.5, 126.4, 126.2, 123.0, 120.0, 62.3, 52.2, 48.4, 31.9, 16.6. HRMS m/z $C_{30}H_{31}N_5O_3S_3$: Calcd. 605.1589, Found 606.1659 $[M+H]^+$. HPLC purity: 96.62%.

4.1.4.8. 4-((4-((2,6-Dimethyl-4-(thiophen-3-yl)phenoxy)thieno[3,2-d]pyrimidin-2-yl)amino)piperidin-1-yl)methyl)benzamide (**18**). White solid, Yield 82%, m.p.: 152–154 °C. 1H NMR (400 MHz, chloroform-*d*) δ 7.73–7.71 (m, 3H), 7.47–7.42 (m, 1H), 7.42–7.36 (m, 2H), 7.33–7.31 (m, 4H), 7.18 (d, J = 5.4 Hz, 1H, C7-thienopyrimidine-H), 6.06–6.04 (m, 2H, CONH₂), 5.00 (d, J = 7.4 Hz, 1H, NH), 3.46 (s, 2H, N–CH₂), 2.71 (d, J = 11.2 Hz, 2H), 2.18 (s, 6H) C, 2.11–1.31 (m, 7H). ^{13}C NMR (100 MHz, chloroform-*d*) δ 169.3, 165.1, 163.5, 160.4, 143.0, 141.8, 134.6, 133.4, 132.0, 131.5, 129.1, 127.3, 126.4, 126.2, 123.1, 120.0, 62.6, 52.2, 48.5, 32.0, 16.6. HRMS m/z $C_{31}H_{31}N_5O_2S_2$: Calcd. 569.1919, Found 570.1995 $[M+H]^+$. HPLC purity: 96.84%.

4.1.4.9. 4-((4-((3,5-Dimethyl-[1,1'-biphenyl]-4-yl)oxy)thieno[3,2-d]pyrimidin-2-yl)amino)piperidin-1-yl)methyl)benzenesulfonamide (**19**). White solid, Yield 75%, m.p.: 130–132 °C. 1H NMR (400 MHz, chloroform-*d*) δ 7.78–7.70 (m, 3H), 7.63–7.60 (m, 2H), 7.44 (t, J = 7.5 Hz, 2H), 7.38–7.32 (m, 5H), 7.18 (d, J = 5.4 Hz, 1H, C7-thienopyrimidine-H), 5.08 (s, 2H, SO₂NH₂), 4.97 (d, J = 7.4 Hz, 1H, NH), 3.46 (s, 2H, N–CH₂), 2.71 (d, J = 11.2 Hz, 2H), 2.20 (s, 6H), 2.02–1.36 (m, 7H). ^{13}C NMR (100 MHz, chloroform-*d*) δ 169.2, 165.1, 161.3, 149.2, 143.5, 140.7, 138.9, 134.6, 132.2, 131.4, 129.7, 128.4, 127.8, 127.2, 123.1, 110.5, 62.9, 52.3, 48.5, 32.2, 16.6. HRMS m/z $C_{32}H_{33}N_5O_3S_2$: Calcd. 599.2025, Found 600.2100 $[M+H]^+$. HPLC purity: 100.00%.

4.1.4.10. 4-((4-((3,5-Dimethyl-[1,1'-biphenyl]-4-yl)oxy)thieno[3,2-d]pyrimidin-2-yl)amino)piperidin-1-yl)methyl)benzamide (**20**). White solid, Yield 88%, m.p.: 143–145 °C. 1H NMR (400 MHz, chloroform-*d*) δ 7.76–7.70 (m, 3H), 7.64–7.59 (m, 2H), 7.45 (t, J = 7.5 Hz, 2H), 7.39–7.30 (m, 5H), 7.18 (d, J = 5.4 Hz, 1H, C7-thienopyrimidine-H), 6.01–6.00 (m, 2H, CONH₂), 4.96 (d, J = 7.4 Hz, 1H, NH), 3.46 (s, 2H, N–CH₂), 2.71 (d, J = 11.2 Hz, 2H), 2.20 (s, 6H), 2.07–1.02 (m, 7H). ^{13}C NMR (100 MHz, chloroform-*d*) δ 169.2, 165.1, 160.5, 149.2, 143.0, 140.7, 138.7, 134.6, 132.0, 131.4, 129.1, 128.7, 127.3, 127.1, 123.1, 62.6, 52.3, 32.0, 16.6. HRMS m/z $C_{33}H_{33}N_5O_2S$: Calcd. 563.2355, Found 564.2426 $[M+H]^+$. HPLC purity: 95.41%.

4.1.4.11. 4-((4-((4'-Methoxy-3,5-dimethyl-[1,1'-biphenyl]-4-yl)oxy)thieno[3,2-d]pyrimidin-2-yl)amino)piperidin-1-yl)methyl)benzenesulfonamide (**21**). White solid, Yield 70%, m.p.: 138–140 °C. 1H NMR (400 MHz, chloroform-*d*) δ 7.82 (d, J = 8.3 Hz, 2H), 7.73 (d, J = 5.4 Hz, 1H, C6-thienopyrimidine-H), 7.53 (d, J = 8.6 Hz, 2H), 7.47–7.45 (m, 2H), 7.40 (d, J = 7.9 Hz, 2H), 7.16 (d, J = 5.4 Hz, 1H, C7-thienopyrimidine-H), 7.02–6.94 (m, 2H), 5.01 (d, J = 7.2 Hz, 1H, NH), 3.48 (s, 2H, N–CH₂), 2.70 (d, J = 12.3 Hz, 2H), 2.18 (s, 6H), 2.11–1.36 (m, 7H). ^{13}C NMR (100 MHz, chloroform-*d*) δ 165.0, 163.5, 160.4,

159.1, 148.7, 144.1, 140.5, 138.3, 134.7, 133.2, 131.3, 129.5, 128.0, 127.3, 126.7, 126.4, 123.0, 114.1, 114.0, 62.3, 55.4, 52.3, 31.9, 16.6. HRMS m/z $C_{33}H_{35}N_5O_4S_2$: Calcd. 629.2130, Found 630.2207 $[M+H]^+$. HPLC purity: 92.74%.

4.1.4.12. 4-((4-((4'-Methoxy-3,5-dimethyl-[1,1'-biphenyl]-4-yl)oxy)thieno[3,2-d]pyrimidin-2-yl)amino)piperidin-1-yl)methyl)benzamide (**22**). White solid, Yield 74%, m.p.: 140–142 °C. 1H NMR (400 MHz, chloroform-*d*) δ 7.81 (d, J = 8.2 Hz, 2H), 7.72 (d, J = 5.3 Hz, 1H, C6-thienopyrimidine-H), 7.54 (d, J = 8.6 Hz, 2H), 7.47 (s, 2H), 7.42 (d, J = 7.9 Hz, 2H), 7.14 (d, J = 5.3 Hz, 1H, C7-thienopyrimidine-H), 7.03–6.98 (m, 2H), 6.02–5.98 (m, 2H, CONH₂), 5.01 (d, J = 7.2 Hz, 1H, NH), 3.48 (s, 2H, N–CH₂), 2.70 (d, J = 12.1 Hz, 2H), 2.18 (s, 6H), 2.11–1.36 (m, 7H). ^{13}C NMR (100 MHz, chloroform-*d*) δ 165.6, 163.2, 160.4, 159.6, 148.1, 143.6, 140.2, 138.7, 134.7, 133.5, 131.3, 129.5, 128.2, 127.3, 127.1, 126.4, 125.8, 123.0, 114.6, 62.2, 55.4, 52.8, 31.9, 16.6. HRMS m/z $C_{34}H_{35}N_5O_3S$: Calcd. 593.2461, Found 594.2532 $[M+H]^+$. HPLC purity: 99.92%.

4.1.4.13. 4-((4-((4'-Fluoro-3,5-dimethyl-[1,1'-biphenyl]-4-yl)oxy)thieno[3,2-d]pyrimidin-2-yl)amino)piperidin-1-yl)methyl)benzenesulfonamide (**23**). White solid, Yield 83%, m.p.: 138–140 °C. 1H NMR (400 MHz, chloroform-*d*) δ 7.84 (d, J = 8.1 Hz, 2H), 7.74–7.71 (m, 2H), 7.50–7.47 (m, 2H), 7.41 (d, J = 8.0 Hz, 2H), 7.21 (s, 2H), 7.16 (d, J = 5.4 Hz, 1H, C7-thienopyrimidine-H), 6.70 (d, J = 1.8 Hz, 1H), 5.08 (s, 2H, SO₂NH₂), 4.95 (d, J = 7.5 Hz, 1H, NH), 3.48 (s, 2H, N–CH₂), 2.70 (d, J = 11.3 Hz, 2H), 2.15 (s, 6H), 1.90–1.40 (m, 7H). ^{13}C NMR (100 MHz, chloroform-*d*) δ 165.0, 160.4, 148.7, 144.1, 143.7, 140.5, 138.3, 134.7, 131.6, 129.9, 129.5, 127.1, 126.6, 126.4, 125.9, 125.8, 123.0, 108.9, 62.3, 52.2, 31.9, 16.5. HRMS m/z $C_{32}H_{32}FN_5O_3S_2$: Calcd. 617.1931, Found 618.2008 $[M+H]^+$. HPLC purity: 97.39%.

4.1.4.14. 4-((4-((4'-Fluoro-3,5-dimethyl-[1,1'-biphenyl]-4-yl)oxy)thieno[3,2-d]pyrimidin-2-yl)amino)piperidin-1-yl)methyl)benzamide (**24**). White solid, Yield 88%, m.p.: 132–135 °C. 1H NMR (400 MHz, chloroform-*d*) δ 7.75–7.73 (m, 4H), 7.50 (d, J = 1.7 Hz, 2H), 7.35 (d, J = 7.9 Hz, 2H), 7.22 (s, 2H), 7.18 (d, J = 5.4 Hz, 1H, C7-thienopyrimidine-H), 6.70 (s, 1H), 5.98–5.96 (m, 2H, CONH₂), 4.92 (d, J = 7.5 Hz, 1H, NH), 3.48 (s, 2H, N–CH₂), 2.72 (d, J = 11.3 Hz, 2H), 2.16 (s, 6H), 1.93–1.43 (m, 7H). ^{13}C NMR (100 MHz, chloroform-*d*) δ 169.2, 165.1, 163.4, 160.4, 148.7, 143.6, 138.3, 134.6, 132.0, 131.6, 129.9, 129.2, 127.3, 126.0, 125.8, 123.2, 108.9, 62.6, 52.2, 32.0, 16.5. HRMS m/z $C_{33}H_{32}FN_5O_2S$: Calcd. 581.2261, Found 582.2370 $[M+H]^+$. HPLC purity: 91.70%.

4.1.4.15. 4-((4-((4'-Cyano-3,5-dimethyl-[1,1'-biphenyl]-4-yl)oxy)thieno[3,2-d]pyrimidin-2-yl)amino)piperidin-1-yl)methyl)benzenesulfonamide (**25**). White solid, Yield 66%, m.p.: 148–150 °C. 1H NMR (400 MHz, chloroform-*d*) δ 7.79–7.62 (m, 7H), 7.35–7.32 (m, 4H), 7.19 (d, J = 5.4 Hz, 1H, C7-thienopyrimidine-H), 5.07 (s, 2H, SO₂NH₂), 4.90 (d, J = 7.4 Hz, 1H, NH), 3.47 (s, 2H, N–CH₂), 2.72 (d, J = 11.2 Hz, 2H), 2.23 (s, 6H), 2.10–1.40 (m, 7H). ^{13}C NMR (100 MHz, chloroform-*d*) δ 169.4, 164.8, 163.7, 161.6, 150.2, 145.8, 136.3,

134.2, 132.5, 132.1, 129.0, 127.6, 127.3, 119.0, 112.4, 62.6, 52.4, 32.1, 16.7. HRMS m/z $C_{33}H_{32}N_6O_3S_2$: Calcd. 624.1977, Found 625.2050 $[M+H]^+$. HPLC purity: 96.65%.

4.1.4.16. 4-((4-((4'-(*Cyano*-3,5-dimethyl-[1,1'-biphenyl]-4-yl)oxy)thieno[3,2-*d*]pyrimidin-2-yl)amino)piperidin-1-yl)methyl)benzamide (**26**). White solid, Yield 74%, m.p.: 156–158 °C. 1H NMR (400 MHz, chloroform-*d*) δ 7.77–7.71 (m, 7H), 7.36–7.33 (m, 4H), 7.20 (d, $J = 5.4$ Hz, 1H), 6.11–5.90 (m, 2H), 4.88 (d, $J = 7.4$ Hz, 1H, NH), 3.47 (s, 2H, N–CH₂), 2.72 (d, $J = 11.3$ Hz, 2H), 2.21 (s, 6H), 1.90–1.42 (m, 7H). ^{13}C NMR (100 MHz, chloroform-*d*) δ 169.1, 165.2, 163.2, 160.4, 150.3, 145.1, 136.5, 134.6, 132.5, 132.0, 129.0, 127.6, 127.3, 127.2, 119.0, 110.7, 62.6, 52.3, 32.0, 16.7. HRMS m/z $C_{34}H_{32}N_6O_2S$: Calcd. 588.2307, Found 589.2382 $[M+H]^+$. HPLC purity: 97.28%.

4.1.4.17. 4-((4-((4'-(*Cyano*-3,5-dimethyl-[1,1'-biphenyl]-4-yl)oxy)thieno[3,2-*d*]pyrimidin-2-yl)amino)piperidin-1-yl)methyl)benzenesulfonamide (**27**). White solid, Yield 74%, m.p.: 140–143 °C. 1H NMR (400 MHz, chloroform-*d*) δ 7.86 (d, $J = 1.5$ Hz, 1H), 7.82 (dd, $J = 7.6, 1.6$ Hz, 1H), 7.76–7.74 (m, 3H), 7.62 (dd, $J = 7.8, 1.5$ Hz, 1H), 7.57 (d, $J = 7.8$ Hz, 1H), 7.37 (d, $J = 7.6$ Hz, 2H), 7.30 (s, 2H), 7.20 (d, $J = 5.4$ Hz, 1H, C7-thienopyrimidine-H), 5.09 (s, 2H, SO₂NH₂), 4.90 (d, $J = 7.2$ Hz, 1H, NH), 3.47 (s, 2H, N–CH₂), 2.73 (d, $J = 11.2$ Hz, 2H), 2.21 (s, 6H), 2.11–1.39 (m, 7H). ^{13}C NMR (100 MHz, chloroform-*d*) δ 169.1, 165.7, 159.3, 150.7, 142.2, 141.6, 136.3, 134.7, 132.3, 131.4, 130.8, 129.6, 129.2, 127.4, 127.0, 123.2, 119.0, 112.9, 62.7, 52.3, 32.1, 16.7. HRMS m/z $C_{33}H_{32}N_6O_3S_2$: Calcd. 624.1977, Found 625.2045 $[M+H]^+$. HPLC purity: 98.93%.

4.1.4.18. 4-((4-((4'-(*Cyano*-3,5-dimethyl-[1,1'-biphenyl]-4-yl)oxy)thieno[3,2-*d*]pyrimidin-2-yl)amino)piperidin-1-yl)methyl)benzamide (**28**). White solid, Yield 83%, m.p.: 140–143 °C. 1H NMR (400 MHz, chloroform-*d*) δ 7.88 (d, $J = 1.6$ Hz, 1H), 7.83 (dd, $J = 7.9, 1.6$ Hz, 1H), 7.75–7.74 (m, 3H), 7.64 (dd, $J = 7.6, 1.5$ Hz, 1H), 7.57 (d, $J = 7.8$ Hz, 1H), 7.35 (d, $J = 7.8$ Hz, 2H), 7.30 (s, 2H), 7.20 (d, $J = 5.4$ Hz, 1H, C7-thienopyrimidine-H), 5.98–5.96 (m, 2H, CONH₂), 4.90 (d, $J = 7.2$ Hz, 1H, NH), 3.48 (s, 2H, N–CH₂), 2.73 (d, $J = 11.2$ Hz, 2H), 2.21 (s, 6H), 2.11–1.39 (m, 7H). ^{13}C NMR (100 MHz, chloroform-*d*) δ 169.2, 165.2, 160.4, 150.0, 142.9, 141.9, 136.3, 134.7, 132.1, 131.4, 130.6, 130.5, 129.6, 129.1, 127.4, 127.1, 123.2, 118.9, 112.9, 62.6, 52.3, 32.0, 26.9, 16.7. HRMS m/z $C_{34}H_{32}N_6O_2S$: Calcd. 588.2307, Found 589.2378 $[M+H]^+$. HPLC purity: 100.00%.

4.1.4.19. 4-((4-((4'-(*Dimethylamino*)-3,5-dimethyl-[1,1'-biphenyl]-4-yl)oxy)thieno[3,2-*d*]pyrimidin-2-yl)amino)piperidin-1-yl)methyl)benzenesulfonamide (**29**). White solid, Yield 66%, m.p.: 172–175 °C. 1H NMR (400 MHz, chloroform-*d*) δ 7.84–7.70 (m, 3H), 7.48 (d, $J = 2.0$ Hz, 2H), 7.43 (d, $J = 8.0$ Hz, 2H), 7.21 (s, 2H), 7.16 (d, $J = 5.4$ Hz, 1H, C7-thienopyrimidine-H), 6.72 (d, $J = 1.8$ Hz, 2H), 5.08 (s, 2H, SO₂NH₂), 5.01 (s, 1H, NH), 3.46 (s, 2H, N–CH₂), 3.02 (s, 6H, NCH₃), 2.71 (d, $J = 11.2$ Hz, 2H), 2.18 (s, 6H), 2.09–1.42 (m, 7H). ^{13}C NMR (100 MHz, chloroform-*d*) δ 165.0, 160.4, 148.7, 144.1, 143.7, 140.5, 138.3, 134.7, 131.6, 129.9, 129.5, 127.1, 126.6, 125.9, 123.0, 108.9, 52.2, 46.9, 42.7, 40.3, 28.4, 16.5.

HRMS m/z $C_{34}H_{38}N_6O_3S_2$: Calcd. 642.2447, Found 643.2524 $[M+H]^+$. HPLC purity: 92.28%.

4.1.4.20. 4-((4-((4'-(*Dimethylamino*)-3,5-dimethyl-[1,1'-biphenyl]-4-yl)oxy)thieno[3,2-*d*]pyrimidin-2-yl)amino)piperidin-1-yl)methyl)benzamide (**30**). White solid, Yield 69%, m.p.: 141–143 °C. 1H NMR (400 MHz, chloroform-*d*) δ 7.84–7.73 (m, 3H), 7.46 (d, $J = 2.0$ Hz, 2H), 7.41 (d, $J = 8.0$ Hz, 2H), 7.20 (s, 2H), 7.16 (d, $J = 5.3$ Hz, 1H, C7-thienopyrimidine-H), 6.74 (d, $J = 2.0$ Hz, 2H), 5.98 (s, 2H, CONH₂), 5.00 (s, 1H, NH), 3.48 (s, 2H, N–CH₂), 3.02 (s, 6H, NCH₃), 2.72 (d, $J = 11.2$ Hz, 2H), 2.18 (s, 6H), 2.04–1.40 (m, 7H). ^{13}C NMR (100 MHz, chloroform-*d*) δ 165.4, 160.9, 148.7, 144.5, 143.7, 140.2, 138.3, 134.4, 132.2, 130.0, 129.2, 127.5, 126.6, 126.0, 125.9, 123.5, 109.2, 52.0, 46.9, 42.9, 39.7, 28.1, 16.5. HRMS m/z $C_{35}H_{38}N_6O_2S$: Calcd. 606.2777, Found 607.2852 $[M+H]^+$. HPLC purity: 96.74%.

4.1.4.21. 4-((4-((4'-(*Dimethylamino*)-3,5-dimethyl-[1,1'-biphenyl]-4-yl)oxy)thieno[3,2-*d*]pyrimidin-2-yl)amino)piperidin-1-yl)methyl)benzenesulfonamide (**31**). White solid, Yield 76%, m.p.: 138–140 °C. 1H NMR (400 MHz, chloroform-*d*) δ 7.86–7.82 (m, 3H), 7.76–7.74 (m, 2H), 7.61 (dd, $J = 7.6, 1.5$ Hz, 1H), 7.54 (d, $J = 7.6$ Hz, 1H), 7.35–7.34 (m, 2H), 7.30 (s, 2H), 7.21 (d, $J = 5.3$ Hz, 1H, C7-thienopyrimidine-H), 5.06 (s, 2H, SO₂NH₂), 5.03 (s, 1H, NH), 3.42 (s, 2H, N–CH₂), 3.02 (s, 6H, NCH₃), 2.70 (d, $J = 11.2$ Hz, 2H), 2.16 (s, 6H), 2.03–1.36 (m, 7H). ^{13}C NMR (100 MHz, chloroform-*d*) δ 169.7, 165.0, 158.9, 150.7, 142.6, 141.6, 137.5, 134.6, 132.3, 131.1, 130.4, 129.2, 127.8, 127.2, 123.1, 119.3, 113.0, 111.8, 62.9, 52.5, 46.9, 42.9, 39.7, 28.1, 16.6. HRMS m/z $C_{34}H_{38}N_6O_3S_2$: Calcd. 642.2447, Found 643.2524 $[M+H]^+$. HPLC purity: 94.44%.

4.1.4.22. 4-((4-((4'-(*Dimethylamino*)-3,5-dimethyl-[1,1'-biphenyl]-4-yl)oxy)thieno[3,2-*d*]pyrimidin-2-yl)amino)piperidin-1-yl)methyl)benzamide (**32**). White solid, Yield 74%, m.p.: 133–135 °C. 1H NMR (400 MHz, chloroform-*d*) δ 7.86–7.81 (m, 3H), 7.76–7.73 (m, 2H), 7.61–7.59 (m, 1H), 7.53 (d, $J = 7.6$ Hz, 1H), 7.32–7.31 (m, 2H), 7.29 (s, 2H), 7.21 (d, $J = 5.3$ Hz, 1H, C7-thienopyrimidine-H), 5.97 (s, 2H, CONH₂), 5.01 (s, 1H, NH), 3.42 (s, 2H, N–CH₂), 3.02 (s, 6H, NCH₃), 2.72 (d, $J = 11.2$ Hz, 2H), 2.16 (s, 6H), 2.00–1.41 (m, 7H). ^{13}C NMR (100 MHz, chloroform-*d*) δ 169.7, 165.0, 159.2, 142.6, 141.7, 137.5, 134.2, 132.3, 131.6, 130.4, 129.2, 127.3, 123.1, 120.5, 113.0, 111.2, 62.9, 52.4, 46.9, 43.2, 39.3, 28.2, 16.6. HRMS m/z $C_{35}H_{38}N_6O_2S$: Calcd. 606.2777, Found 607.2852 $[M+H]^+$. HPLC purity: 95.29%.

4.2. *In vitro* anti-HIV activities assays

The anti-HIV activity and cytotoxicity of the novel synthesized compounds were evaluated using the 3-(4,5-dimethylthiazol-2-yl)-2,5-diphenyltetrazolium bromide (MTT) method in MT-4 cell cultures as described previously^{19,20}. Firstly, stock solutions (10 × final concentration) of the compounds were added in 25 μ L volumes to two series of triplicate wells with the aim to allow simultaneous evaluation of their effects on mock- and HIV-infected cells. With a Biomek 3000 robot (Beckman Instruments, Fullerton, CA, USA), serial 5-fold dilutions of the test compounds were made directly in flat-bottomed 96-well microtiter trays, including untreated control HIV-1 and mock-infected cell

samples for each sample. Wild-type and mutant HIV-1 strains stock (50 μ L at 100–300 CCID₅₀) or culture medium was added to either the infected or mock-infected wells of the microtiter tray. Mock-infected cells were used to evaluate the effect on uninfected cells to assess compounds cytotoxicity. Exponentially growing MT-4 cells were centrifuged for 5 min at 1000 rpm (Eppendorf 5424, Hamburg, Germany) and then supernatant was discarded. The MT-4 cells were resuspended at 6×10^5 cells/mL, and 50 μ L aliquots were transferred to the microtiter tray wells. At 5 days after infection, the viability of mock- and HIV-infected cells was determined spectrophotometrically by means of MTT assay.

The MTT assay is based on the reduction of yellow-colored MTT (Acros Organics, Geel, Belgium) by mitochondrial dehydrogenase of metabolically active cells to form a blue-purple formazan. The absorbances were read in an eight-channel computer-controlled photometer at the wavelengths of 540 and 690 nm. All data were calculated using the median optical density (OD) value of three wells. The EC₅₀ was defined as the concentration of the test compound affording 50% protection from viral cytopathogenicity. The CC₅₀ was defined as the compound concentration that reduced the absorbance (OD₅₄₀) of mock-infected cells by 50%.

4.3. Recombinant HIV-1 RT inhibitory assays

The HIV-1 RT inhibition assay was tested with an RT assay kit (Roche, Basel, Switzerland)²¹. Briefly, the reaction mixture containing HIV-1 RT enzyme, reconstituted template and viral nucleotides [digoxigenin (DIG)-dUTP, biotin-dUTP and dTTP] in the incubation buffer with or without inhibitors was incubated for 1 h at 37 °C. Then, the reaction mixture was transferred to a streptavidin-coated microtitre plate (MTP) and incubated for 2 h at 37 °C. The biotin-labeled dNTPs were incorporated into the cDNA chain in the presence of RT. The unbound dNTPs were washed with washing buffer, and anti-DIG-POD was added to the MTPs.

After incubation for additional 1 h at 37 °C, the DIG-labeled dNTPs incorporated in cDNA were bound to the anti-DIG-POD antibody. The unbound anti-DIG-PODs were washed out and the peroxide substrate (ABST) solution was added to the MTPs. The absorbance of the sample was determined at OD₄₀₅ using a microtiter plate ELISA reader (Multiskan Sky, Waltham, MA, USA). The percentage inhibitory activity of RT inhibitors was calculated using the following Eq. (1):

$$\text{Inhibition (\%)} = \frac{(\text{OD value with RT but without inhibitors} - \text{OD value with RT and inhibitors})}{(\text{OD value with RT and inhibitors} - \text{OD value without RT and inhibitors})} \quad (1)$$

The IC₅₀ values correspond to the concentrations of the inhibitors required to inhibit biotin-dUTP incorporation by 50%.

4.4. Molecular modelling studies

4.4.1. Models preparation

The X-ray crystal structure of HIV-1 WT RT (PDB code: 6c0n), HIV-1 K103N RT (PDB code: 6c0o) and HIV-1 RES056 RT (PDB code: 6c0r), respectively corresponding to the X-ray crystallographic structure of the WT, K103N and RES056 RT in complex with the NNRTIs **K-5a2** were chosen to build up the initial models

for compound **26**. The atom–atom pair fitting procedure implemented in PyMOL V1.7 (<https://pymol.org/>) was applied to manually dock compound **26** into the NNRTIs binding site, according to the high molecular similarity of the crystallographic and simulated ligands.

4.4.2. Molecular dynamics simulations

Amber16 was used to explore the stability of compound **26** into the NNRTI binding site of the three simulated HIV-1 RT models by means of unbiased MD simulations. The Amber ff99SB-ILDN force field²² was used for the protein and protonation states at physiological pH were optimized in accordance to the pK_a values estimated by Propka^{23,24}. The general Amber force field (GAFF)²⁵ was used to parameterize the ligand and partial charges were derived at the B3LYP/6-31G(d) level of theory with Gaussian 09²⁶, after preliminary optimization of the molecular structure, by using the restrained electrostatic potential (RESP) fitting method implemented in Antechamber.

The complex was then solvated with a truncated octahedral (TIP3P) water box with a layer of 20 Å and neutralized by adding Cl[−] counterions. The position of the conserved water molecule (HOH 817 in 6c0n, 824 in 6c0o and 736 in 6c0r), which mediates H-bonding interactions between the protonated pyrimidine nitrogen of the ligand and the protein backbone oxygen atoms of K/N103 and P236, was retained during generation of the starting complexes although it was revealed to be not stable along the simulation.

A stepwise minimization involving firstly all hydrogen atoms, then water molecules, and finally all the system with a maximum number of minimization cycles of 10,000 (the first 2000 by using the steepest descent method and the rest with conjugate gradient) for the latter stage was applied to the three pre-generated complexes. Prior to MD simulation, heating and equilibration of the system from 0 to 300 K was accomplished in six steps, the first being performed at constant volume and the rest at constant pressure. Harmonic restraints with a force constant of 10 kcal/mol/Å were applied during heating to some crucial interactions involving compound **26**, the conserved water molecule and HIV-1 RT during equilibration in order to avoid artefactual structural changes on the pre-generated binding mode. These restraints were gradually reduced at 5 kcal/mol/Å during the 5 ns of equilibration and totally eliminated in the first 10 ns of MD production. The SHAKE algorithm was applied to constrain bonds involving hydrogen atoms. Periodic boundary conditions at constant volume were imposed on the systems during the MD simulations. Cut-off for the non-bonded interactions was set to 10 Å. The electrostatic interactions beyond the cut-off within the periodic box were computed by applying the Particle Mesh Ewald (PME) method. Langevin dynamics with a collision frequency of 1.0/ps was applied for temperature regulation during the heating. A total of 100 ns of unrestrained MD simulation at constant volume and temperature (300 K) using the weak-coupling algorithm with a time constant of 10.0 were run for the three pre-equilibrated systems. The time step for saving of trajectory was set to 2 ps.

Finally, trajectories for the unrestrained part of the three MD runs were generated and analysed by using the CPPTRAJ module of Amber. A total of 20,000 frames were collected for each simulated system. Complexes stability during MD simulation was evaluated by means of RMSD analysis for the NN binding site (residues 8 Å around the ligand), and for the ligand itself. The stability of some relevant ligand–protein interactions was also analysed.

4.4.3. Binding free energy calculations

The contributions to the binding free energy were calculated for the three complexes according to the GB method implemented in the MMGBSA.py module of Amber [S14]. The method allows calculating the free energy (G) of each species (ligand, protein and complex) as the sum of enthalpic (gas-phase) (E_{gas}), solvation (G_{solv}) and entropy (S) terms, according to Eq. (2):

$$G = E_{\text{gas}} + G_{\text{solv}} - TS = E_{\text{int}} + E_{\text{elect}} + E_{\text{vdW}} + G_{\text{solv, pol}} + G_{\text{solv, n-pol}} - TS \quad (2)$$

where E_{int} , E_{elect} and E_{vdW} are the internal, Coulomb, and van der Waals energy terms and account, respectively, for bonded, polar, and non-polar energy contributions in the gas-phase, $G_{\text{solv, pol}}$ is the polar contribution to solvation free energy evaluated by using the Generalized-Born solvation method, and $G_{\text{solv, n-pol}}$ accounts for non-polar contributions to solvation free energy and was computed linearly to the solvent-accessible surface area (SASA; Eq. (3)).

$$G_{\text{solv, n-pol}} = \gamma \text{SASA} + b \quad (3)$$

where γ is the surface tension (set to 0.0072 kcal/mol/Å²) and b is a correction term which is assumed to be zero in the present calculation.

All these contributions were calculated for complex, receptor and ligand and the binding free energy (G_{bind}) was evaluated as the difference for the three species (Eq. (4))

$$\Delta G_{\text{bind}} = \langle G_{\text{complex}} \rangle_{\text{traj}} - \langle G_{\text{receptor}} \rangle_{\text{traj}} - \langle G_{\text{ligand}} \rangle_{\text{traj}} \quad (4)$$

where $\langle G_x \rangle_{\text{traj}}$ accounts for the average value for each species (x : complex, receptor, ligand) determined for an ensemble of 100 snapshots taken from the last 30 ns of MD trajectory of the complexes within the framework of the single-trajectory approach. The vibrational entropy term (S) was not determined.

Acknowledgments

We gratefully acknowledge financial support from the Key Project of NSFC for International Cooperation (No.81420108027, China), the National Natural Science Foundation of China (NSFC Nos. 81273354, 81573347, 81903453), Young Scholars Program of Shandong University (YSPSDU No. 2016WLJH32, China), Shandong Provincial Natural Science Foundation (ZR2019BH011, China), China Postdoctoral Science Foundation (2018M640641, 2019T120596), Key research and development project of Shandong Province (No. 2017CXGC1401, China) and KU Leuven (GOA 10/014, Belgium). The technical assistance of Mr. Kris Uyttersprot and Mrs. Kristien Erven, for the HIV experiments is gratefully acknowledged. T.G. thanks the Spanish Government (MINECO Project SAF2017-881074-R, AEI/FEDER, UE), and Generalitat de Catalunya (2017SGR1746, Spain) for the financial support. The Barcelona Supercomputer Center (BSC) is also acknowledged for providing access to supercomputation resources.

Author contributions

Dongwei Kang, Peng Zhan and Xinyong Liu conceived the project. Dongwei Kang, Da Feng, Fenju Wei and Yanying Sun finished the compounds synthesis and structure confirmation.

Dongwei Kang, Jinmi Zou, Tong Zhao and Samuel Desta designed the pharmacokinetics and acute toxicity experiment. Dongwei Kang and Boshi Huang performed the data analysis. Tiziana Ginex performed the molecular modeling study. Eeik De Clercq and Christophe Pannecouque performed the activity test. Peng Zhan and Xinyong Liu provided the resources, supervision and funding assistance.

All authors critically evaluated the manuscript prior to submission.

Conflicts of interest

The authors have no conflicts of interest to declare.

Appendix A. Supporting information

Supplementary data to this article can be found online at <https://doi.org/10.1016/j.apsb.2019.08.013>.

References

- Shattock RJ, Warren M, McCormack S, Hankins CA. AIDS. Turning the tide against HIV. *Science* 2011;**333**:42–3.
- Guo H, Zhuang X, Qian K, Sun L, Wang X, Li H, et al. Prodrug design, synthesis and pharmacokinetic evaluation of (3'*R*,4'*R*)-3-hydroxymethyl-4-methyl-3',4'-di-*O*-(*S*)-camphanoyl-(+)-*cis*-khel-lactone. *Acta Pharm Sin B* 2012;**2**:213–9.
- Zhan P, Chen X, Li D, Fang Z, de Clercq E, Liu X. HIV-1 NNRTIs: structural diversity, pharmacophore similarity, and implications for drug design. *Med Res Rev* 2013;**33**(Suppl 1):E1–72.
- Bec G, Meyer B, Gerard MA, Steger J, Fauster K, Wolff P, et al. Thermodynamics of HIV-1 reverse transcriptase in action elucidates the mechanism of action of non-nucleoside inhibitors. *J Am Chem Soc* 2013;**135**:9743–52.
- Namasivayam V, Vanangamudi M, Kramer VG, Kurup S, Zhan P, Liu X, et al. The journey of HIV-1 non-nucleoside reverse transcriptase inhibitors (NNRTIs) from lab to clinic. *J Med Chem* 2019;**62**:4851–83.
- Beyrer C, Pozniak A. HIV drug resistance—an emerging threat to epidemic control. *N Engl J Med* 2017;**377**:1605–7.
- Xu HT, Asahchop EL, Oliveira M, Quashie PK, Quan Y, Brenner BG, et al. Compensation by the E138K mutation in HIV-1 reverse transcriptase for deficits in viral replication capacity and enzyme processivity associated with the M184I/V mutations. *J Virol* 2011;**85**:11300–8.
- Huang B, Chen W, Zhao T, Li Z, Jiang X, Ginex T, et al. Exploiting the tolerant region I of the non-nucleoside reverse transcriptase inhibitor (NNRTI) binding pocket: discovery of potent diarylpyrimidine-typed HIV-1 NNRTIs against Wild-Type and E138K mutant virus with significantly improved water solubility and favorable safety profiles. *J Med Chem* 2019;**62**:2083–98.
- Li D, Zhan P, de Clercq E, Liu X. Strategies for the design of HIV-1 non-nucleoside reverse transcriptase inhibitors: lessons from the development of seven representative paradigms. *J Med Chem* 2012;**55**:3595–613.
- Kang D, Wang Z, Chen M, Feng D, Wu G, Zhou Z, et al. Discovery of potent HIV-1 non-nucleoside reverse transcriptase inhibitors by exploring the structure–activity relationship of solvent-exposed regions I. *Chem Biol Drug Des* 2019;**93**:430–7.
- Zhan P, Pannecouque C, de Clercq E, Liu X. Anti-HIV drug discovery and development: current innovations and future trends. *J Med Chem* 2016;**59**:2849–78.
- Kang D, Zhang H, Wang Z, Zhao T, Ginex T, Luque FJ, et al. Identification of dihydrofuro[3,4-*d*]pyrimidine derivatives as novel HIV-1 non-nucleoside reverse transcriptase inhibitors with promising

- antiviral activities and desirable physicochemical properties. *J Med Chem* 2019;**62**:1484–501.
13. Zuo X, Huo Z, Kang D, Wu G, Zhou Z, Liu X, et al. Current insights into anti-HIV drug discovery and development: a review of recent patent literature (2014–2017). *Expert Opin Ther Pat* 2018;**28**:299–316.
 14. Kang D, Fang Z, Li Z, Huang B, Zhang H, Lu X, et al. Targeting the hydrophobic channel of NNIBP: discovery of nove. *J Med Chem* 2016;**59**:7991–8007.
 15. Kang D, Fang Z, Huang B, Lu X, Zhang H, Xu H, et al. Structure-based optimization of thiophene[3,2-*d*]pyrimidine derivatives as potent HIV-1 non-nucleoside reverse transcriptase inhibitors with improved potency against resistance-associated variants. *J Med Chem* 2017;**60**:4424–43.
 16. Yang Y, Kang D, Nguyen LA, Smithline ZB, Pannecouque C, Zhan P, et al. Structural basis for potent and broad inhibition of HIV-1 RT by thiophene[3,2-*d*]pyrimidine non-nucleoside inhibitors. *eLife* 2018;**7**:e36340.
 17. Zhou Z, Liu T, Wu G, Kang D, Fu Z, Wang Z, et al. Targeting the hydrophobic channel of NNIBP: discovery of novel 1,2,3-triazole-derived diarylpyrimidines as novel HIV-1 NNRTIs with high potency against wild-type and K103N mutant virus. *Org Biomol Chem* 2019;**17**:3202–17.
 18. Zhou Z, Liu T, Kang D, Huo Z, Wu G, Daelemans D, et al. Discovery of novel diarylpyrimidines as potent HIV-1 NNRTIs by investigating the chemical space of a less explored “hydrophobic channel”. *Org Biomol Chem* 2018;**16**:1014–28.
 19. Pauwels R, Balzarini J, Baba M, Snoeck R, Schols D, Herdewijn P, et al. Rapid and automated tetrazolium-based colorimetric assay for the detection of anti-HIV compounds. *J Virol Methods* 1988;**20**:309–21.
 20. Pannecouque C, Daelemans D, de Clercq E. Tetrazolium-based colorimetric assay for the detection of HIV replication inhibitors: revisited 20 years later. *Nat Protoc* 2008;**3**:427–34.
 21. Suzuki K, Craddock BP, Okamoto N, Kano T, Steigbigel RT. Poly A-linked colorimetric microtiter plate assay for HIV reverse transcriptase. *J Virol Methods* 1993;**44**:189–98.
 22. Hornak V, Abel R, Okur A, Strockbine B, Roitberg A, Simmerling C. Comparison of multiple Amber force fields and development of improved protein backbone parameters. *Proteins* 2006;**65**:712–25.
 23. Lindorff-Larsen K, Piana S, Palmo K, Maragakis P, Klepeis JL, Dror RO, et al. Improved side-chain torsion potentials for the Amber ff99SB protein force field. *Proteins* 2010;**78**:1950–8.
 24. Søndergaard CR, Olsson MH, Rostkowski M, Jensen JH. Improved treatment of ligands and coupling effects in empirical calculation and rationalization of pK_a values. *J Chem Theory Comput* 2011;**7**:2284–95.
 25. Olsson MH, Søndergaard CR, Rostkowski M, Jensen JH. PROPKA3: consistent treatment of internal and surface residues in empirical pK_a predictions. *J Chem Theory Comput* 2011;**7**:525–37.
 26. Wang J, Wolf RM, Caldwell JW, Kollman PA, Case DA. Development and testing of a general amber force field. *J Comput Chem* 2004;**25**:1157–74.